This is to certify that the

thesis entitled

Thermal and Mechanical Properties of
Fly Ash - Calcium Carbonate Refractory Materials

presented by

Chiu Chin-Chen

has been accepted towards fulfillment
of the requirements for
Master M.M.
_____ degree in _____

Eldon Case

Major professor

Date 5/15/87

THERMAL AND MECHANICAL PROPERTIES OF FLY ASH -- CALCIUM CARBONATE REFRACTORY MATERIAL

By

Chin-Chen Chiu

A THESIS

Submitted to
Michigan State University
in partial fulfillment of the requirements
for the degree of

MASTER OF SCIENCE

Department of Metallurgy, Mechanics,
and Materials Science

1987

ABSTRACT

THERMAL AND MECHANICAL PROPERTIES OF FLY ASH
-- CALCIUM CARBONATE REFRACTORY MATERIAL

By

Chin-Chen Chiu

The flexural strength of seven different compositions of fly ash-calcium carbonate refractory material was measured at temperatures up to 400 degrees Celsius using the three point bend test. The room temperature compressive strength and the resistance to water attack were also studied. The experimental results indicate that the mechanical strength decreases with increasing temperature and calcium carbonate content. The proper addition of calcium carbonate can improve the resistance to water attack.

Thermal properties studied in this research include thermal shock, thermal expansion, specific heat, and thermal conductivity. Thermal conductivity data obtained by hot-wire technique show that the conductivity decreases with the increasing temperature and supports the postulate that this kind of refractory is a good thermal insulator.

ACKNOWLEDGEMENTS

I am deeply indebted to my advisor, Dr. Eldon Case, for his positive guidance, continuous encouragement, and constructive evaluations. I am also grateful to the Lansing Board of Water and Light for their finanical support and the assistance they have provided to me throughout my study.

To my friend, Jack Chou, I would like to express my gratitude for his valuable suggestions. A special thanks to Christine Horng, who, with her typing and editorial skills, was instrumental in helping me compile this document.

TABLE OF CONTENTS

LIST OF TABLES

LIST OF FIGURES

INTRODUCTION

The measurements of mechanical strength and thermal properties are basic procedures in most refractory research. They are also standard quality control measures in refractory plants. The strength and thermal properties of a new refractory may indicate if the processing techniques are suitable or if the new composition is acceptable. For example, an unsuitable composition may result in weak bonding in the refractory which may result in a reduction in strength.

The fly ash-calcium carbonate refractory material discussed in this report was formed from the Lansing Board of Water and Light by-products of fly ash and limestone sludge. (For brevity, the "as-fired" form of the material is referred to as "LBWL product"). The production of the LBWL product involved using sodium silicate as a binding phase. A microwave was used to solidify the unfired product.

The principle objective of this research was to characterize the mechanical and the thermal properties of LBWL product. In addition to the study of the mechanical and thermal properties of LBWL product, some additional investigations were also performed on the raw materials that comprise the LBWL product, including fly ash, limestone

sludge, and water glass. In short, this research includes twelve catagories as follows : (1) mechanical properties testing, such as bend strength and cold-crushing strength; (2) measurement of the thermal conductivity and thermal expansion of LBWL products; (3) evaluation of thermal shock of LBWL products; (4) x-ray diffraction analysis of crystalline phases present in limestone sludge; (5) x-ray diffraction analysis of crystalline phases in the fly ash powders and morphological observation of the fly ash powders by optical microscope and scanning electron microscope; (6) measurement of the temperature of LBWL product during microwave processing; (7) manufacture of LBWL products; (8) crystallographical and morphological analysis of LBWL products; (9) measurement of the density and the water absorption of LBWL products; (10) study of the resistance of LBWL product to water attack; (11) measurement of the specific heat of LBWL product; and (12) measurement of the Young's modulus and the acoustic dampening properties of the LBWL product.

In addition, the mechanical and thermal properties of the LBWL product were compared to those of dry wall (gypsum board).

EXPERIMENTAL PROCEDURES AND TECHNIQUES

I. X-ray Diffraction Analysis of Sludge

The sludge received from Board of Water and Light on December 20, 1985 was prepared using several methods. First, the water-like sludge was put in a ceramic ovenware container, then put in a drying oven (serial No. 16 A-G-2, Precision Scientific Co. Chicago, Illinois) and heated to 45 degrees Celsius. The temperature was read from a mecury-in-glass thermometer mounted through the top of the furnace. After 16 hours, the sludge was removed and ground into a powder with a porcelain mortar and pestle. The sludge powder obtained in this way was used for further testing.

Two samples of sludge powder, each weighing about ten grams, were placed in porcelain crucibles (Coors, USA) to be heat-treated. The first sample was heated to 400 degrees Celsius for 3 hours and the second sample was heated to 800 degrees Celsius for 3 hours. A resistance-heating furnace (Lingberg, Type 51442, Watertown, Wisconsin) was used and samples were heated in air.

Before operating the x-ray machine, the sludge sample was pressed into a grooved rectanglar aluminum stage. The

specimen was then flattened using a glass slide. The thickness of the compacted powder specimen was estimated to be approximately 0.5 mm. The operating conditions of the x-ray machine were as follows: (1) the diffraction angle 2θ ranged from 15 degrees Celsius to 55 degrees Celsius; (2) the counts per second (C.P.S) were set at 1000 ; (3) the chart speed was 1 inch/minute; (4) the diffractometer speed was set at 0.25 θ per minute.

The diffraction patterns of the sludge were also compared with the diffraction patterns from both pure calcium carbonate (Analytical Reagent, Mallinckrodt Inc., Paris, Kentucky) and calcined calcium carbonate. The calcination of the calcium carbonate was performed in air in a resistance-heating furnace at 800 degrees for 14 hours. The operating conditions of the x-ray machine for both specimens of calcium carbonate were the same as that for the sludge specimen.

II. Preparation of Fly Ash

The fly ash received from Board of Water and Light was prepared using five different methods: (1) reheating in air; (2) magnetic separation; (3) chemical reaction; (4) treatment by organic liquid; (5) heating in a sealed fused silica tube.

(1) Heating in Air

Four samples of fly ash, roughly ten grams each, were

placed in alumina crucibles. The samples were reheated in a resistance-heating furnace at settings of 300, 500, 800, and 1200 degrees Celsius, respectively. According to the time schedule given in table 1, portions of each sample, each about 2 grams, were taken out. Then they were analyzed by x-ray diffraction and observed by SEM (see the section "Analysis of fly ash").

(2) Magnetic Separation

Some fly ash was placed in a ceramic container. A horseshoe magnet, covered with plastic wrap, was placed above the fly ash. The magnetic particles were drawn to the magnet and removed. The magnet was covered with plastic wrap so that when the particles were drawn to the magnet they could be removed from the magnet by simply removing the plastic. Contamination was also reduced by this process.

To further separate the magnetic from the nonmagnetic particles, the particle fraction collected by the magnet was soaked in alcohol solution (water/ethanol = 4/1). The magnet was then moved fairly quickly across the solution and the highly magnetic particles were drawn from the solution. The particles were placed in a beaker and dried in air in a drying oven at about 110 degrees Celsius for 2 hours. After drying, some of the magnetic particles were analyzed by x-ray diffraction, observed by SEM, and etched by HF + HCl solution (see the section "Chemical Reaction") for 15 minutes. The

processing procedure is described in the following section, entitled "Chemical Reaction". The other specimens were reheated at 800 degrees Celsius for 6 hours (see the section "Analysis of fly ash").

(3) Chemical Reaction:

Samples of fly ash, each weighing two grams, were mixed with chemical reagents according to Table 2. When the time indicated in Table 2 had elapsed, a large amount of tap water was added to the beaker in order to stop the reaction. A filter paper (Whatman, 100 circles, 1. qualitative) was used to retain the fly ash. The filter paper, with the ash in place, was then flushed with water about five to ten times to wash out the residual chemical reagent. The fly ash was then dried in air at 110 degrees C for 6 hours. Lastly, the fly ash was observed by SEM (see the section "Analysis of fly ash").

(4) Treatment by Organic Liquid:

Five grams of fly ash were put in a solution of 10 c.c. water and 1 c.c. organic liquid (60 percent methyl ethyl, ketone peroxide in dimethyl phthalate). The organic liquid, which was not miscible with water, formed small droplets and a thin film on the top of the solution. It was observed that black particles became attached to the organic liquid droplets. Droplets containing the black particles were

removed using a small ladle and put in a beaker. The beaker was then dried in air in a drying oven at 110 degrees Celsius for 3 hours. Following the drying treatment, a sample of the black particles was coated with a Pt-Pd alloy via vacuum deposition. The black particles were then observed in the SEM.

(5) Heating in a Sealed Tube:

Twenty eight grams of fly ash were dried at 200 degrees Celsius for 15 minutes in air in a resistance-heating furnace. After drying, 25.8389 grams of fly ash were placed in an open crucible and 1.0000 gram was placed in a 0.7 cm diameter fused silica tube. The tube was evacuated by first sealing off one end of the tube using a oxyacetalyne torch. A rotary pump was used to reduce the gas pressure in the tube to approximately 10^{-2} torr, and then the other end of the tube was sealed using the oxyacetalyne torch.

The sample in the open crucible and the sample in the sealed evacuated tube were then heated together at 800 degrees Celsius for 16 hours in air in a resistance-heating furnace. The weight loss for the two different specimens was then calculated.

Table 1. Time Schedule of Fly Ash Reheated in Resistance-heating Furnace

Temperature (degrees C.)	Heating duration (hours)		
300	30	27.5	
500	4	8	49
800	3	17	49
1200	6.5		

Table 2. Chemical Reagents Used in Fly Ash Reaction Studies

Chemical reagents	Concentration (by volume)	Time allowed for reaction
Phosphoric acid(85%) + Tap water	50% + 50%	14 hours
Water glass* + Tap water	50% + 50%	14 hours
HF(48%) + HCl(38%) + Tap water	33% + 33% + 33%	15 minutes

* JM grade, E. I. Du Pont Nemours & Co. Composition: 29.6% SiO_2, 9.10% Na_2O. Weight ratio of SiO_2 to Na_2O : 3.25

Table 3. Fly Ash Analysis Techniques

Techniques	Types of prepared fly ash
Analysis by x-ray diffraction	Original fly ash Reheated fly ash Magnetic fly ash
Observation by SEM	Original fly ash Reheated fly ash* Magnetic fly ash** Chemically reacted fly ash Black particles in fly ash

* Only the fly ash reheated at 800 degrees Celsius for 49 hours and at 1200 degrees Celsius for 6.5 hours were observed in the SEM.

** Includes the magnetic fly ash etched in HF solution.

III. Analysis of Fly Ash

After the preparation described in the previous section, the different types of prepared fly ash were analyzed by x-ray diffraction or SEM. Table 3 indicates the prepared fly ash which was analyzed.

In SEM observation (Hitachi model 415A) an aluminum stub (1.2 cm in diameter and 0.4 cm in height) was prepared for each sample. The top surface of the stub was covered with a thin coating of silver paint. Fly ash was spread on the painted surface and the paint was allowed to dry. The fly ash particles were thus fixed in place by the dried conductive paint. To further ensure the surface electrical conductivity required for SEM examination of non-conducting specimens, the specimen stubs with the fly ash in place were coated with Pt-Pd alloy by a vacuum deposition. The conditions of vacuum deposition were (1) pressure: $2 * 10^{-5}$ torr; (2) filament voltage: 35 volts; (3) distance from filament to specimen: about 10 cm (the vacuum deposition apparatus used a Series # 90982, Welch Scientific Company, Skokie, Illinois). After coating, the stub was placed in the SEM chamber and manual operating procedures were followed.

IV. Manufacture of Specimen (LBWL Product)

LBWL specimens used in this study were microwave processed at the Lansing Board of Water and Light facilities.

Several specimens of compositions 1, 2, and 3 used early in this study were processed by Board of Water and Light personnel, but additional specimens of each of the seven LBWL product compositions were processed at the Lansing Board of Water and Light facilities by Michigan State University personnel, including the author. After processing, all specimens were taken to Michigan State University for testing and analysis.

(1) Measurement of Specific Heat and Specimen Temperature

In order to characterize the processing conditions of the LBWL product, the temperature of the specimens during the microwave heating was established. In order to calculate the processing temperature, the specific heat of the LBWL product was determined using standard calorimetric procedures. The measured specific heat was then used in the experimental determination of the specimen temperature during the microwave processing treatment.

Specimens of LBWL product were received from Board of Water and Light that had been solidified by microwaving. In general, the temperature of the specimens during mircowave processing is considered to be an important parameter. Therefore, in order to estimate the processing temperature, the specific heat of the specimens was calculated first as follows:

First, the room temperature T1 was determined with a

mercury-in-glass thermometer having a range from 0 to 200 degrees Celsius. LBWL specimens (which had been fractured in the strength testing) were dried in air in an oven at 110 degrees Celsius for one half hour. The specimens, each of which weighed about 40 grams, were weighed using an electronic balance and then dried for an additional hour at temperature T2. Temperature T2 was read from a mercury-in-glass thermometer mounted on the top of the drying oven. About 400 grams of water was placed in a 1000 c.c. beaker which was partially insulated by a styrofoam container. The mass of the water was determined using an electronic balance and the temperature, T3, of the water was measured using a Beckmann thermometer having a range covering 6 degrees Celsius with 0.01 degree Celsius divisions.

The heated specimens were quickly placed into the water in the beaker and the water temperature, T4, was determined using the Beckmann thermometer.

The specific heat, Hs, of the LBWL specimens were calculated using equation 1,

$$(T4 - T3) * Ww * Hw = (T2 - T4) * Ws * Hs \qquad (1)$$

Ww = weight of water

Hw = specific heat of water

Ws = weight of specimen

Hs = specific heat of specimen

T2 = temperature of hot specimens

T3 = temperature of water before

hot specimens were put into the beaker

T4 = temperature of water after hot specimens were put into the beaker

In order to check the validity of the experimental procedure, a pure copper specimen with a specific heat of 0.0919 calorie/gram C [1] was tested in the same manner to see if the experimental value for specific heat was the same as the theoretical value. The pure copper, a tensile test specimen which weighed 50.50 grams, was obtained from a laboratory where the recrystallization of pure copper was being studied. The experimental value of the pure copper was calculated according to the same procedures as for LBWL product.

The temperature of the LBWL product during microwaving was calculated using equation (1) and the measured value of specific heat for the LBWL product. Forty gram specimens were heated in the Board of Water and Light microwave for 10 minutes using a microwave power setting of 470 watts. Then the values of T2, the temperature of the specimens during the microwave processing, were recorded.

(2) Processing of LBWL Product

Fly ash-calcium carbonate refractory material (LBWL product) was produced using fly ash, water glass, and other

ingredients. The compositions of the LBWL products are listed in Table 4.

The processing of the LBWL products began with mixing the raw materials. For compositions 1, 2, 3, 4, 6, and 7, first 200 grams of fly ash was mixed with the other solid ingredients in a beaker. The weight of the ingredients used was determined according to the Table 4. At the same time water and water glass were mixed together in another beaker. The water/waterglass mixture was then combined with the solid ingredients and mixed vigorously in a plastic pan for a minimum of 20 minutes. The final clay-like mixture was placed in a sandwich saver approximately 12.5 cm * 12.5 cm * 3.5 cm, in which 80 to 120 holes were drilled at random spatial positions. Each hole was approximately 0.3 cm in diameter. The holes were punched on the bottom of the plastic tray so that the moisture could evaporate out easily. The mixture was flattened using a metal spatula and set in a microwave for 5 minutes (set at medium range). The hardened product was then removed from the microwave, taken out of the container and heated again for 10 minutes.

In making the specimens for the measurement of thermal conductivity, the hardened product was not removed from the container at once. Since thicker specimens were required for the thermal conductivity testing than for the strength testing, approximately 300 grams of clay-like mixture was added on the top of the hardened product. Then the layered green body was set in a microwave (brand: Quasar Japan) for another 5 minutes. Finally, the specimen was removed from

the microwave, taken from the container and heated for an additional 10 minutes.

For composition 5, the fly ash was mixed first with the phosphoric acid solution which was diluted with water as given in Table 4. After waiting for an hour, water glass was added to the other reagents and the entire mixture was heated in the microwave as described above.

Table 4. The Composition of Various LBWL Products

Specimen number	Fly ash*	Water glass	Dry sludge	Tap water	Potassium phosphate	Sodium phosphate	Phosphoric acid
1	100	50.2		20.4	4.9		
2	100	50	25	30		5	
3	100	45.4	9	22.7		3.6	
4	100	50		20			
5	100	50		20			0.75(c.c.) (85 %)
6	100	50	21	20			
7	100	50	10	20			

* The 100 grams of fly ash was used as reference. Except where otherwise noted, all amounts are in grams. Compositions 1, 2, 3 were produced by Board of Water and Light.

V. Analysis of Specimen (LBWL Product)

The following analyses were performed on specimens of the LBWL product:

(1) X-ray diffraction and SEM investigation

(2) Measurement of mass density

(3) Three point bend test

(4) Examination of LBWL product reheated at elevated temperature

(5) Compression test

(6) Measurement of thermal conductivity

(7) Measurement of thermal expansion

(8) Evaluation of thermal shock

(9) Measurement of Young's modulus and acoustic damping capacity

(1) X-ray Diffraction and SEM Investigation

For the x-ray diffraction analysis, the microwave processed LBWL product was ground into a powder with a porcelain mortar and pestle. The diffraction results were obtained using the same procedure as that used for the fly ash.

The fracture surfaces of specimens broken in the three point bend testing were coated with a Pt-Pd alloy in the vacuum depositer under the same conditions used to coat the fly ash specimens. Prior to coating in the vacuum depositer, the specimens had been attached to cylindrical aluminum stubs

1.2 cm in diameter and 0.4 cm in height using an organic glue.* The microstructure of these fracture surfaces was observed in the SEM.

(2) Measurement of Density

In order to measure the specimen volume, the LBWL product was cut into a rectangle (12 cm * 1.3 cm * 1.3 cm), ground with a rotating belt sander and measured using a metric dial caliper. The weight of the specimens was determined to within $\pm$ 0.01 grams using a Mettler balance. Then the mass density of the LBWL product was calculated as follows:

$$\text{Density} = \text{Weight} / \text{Volume}$$

(3) Three Point Bend Test

For each of the seven LBWL product compositions listed in Table 4 and for the dry wall**, modulus of rupture tests were done: (A) at room temperature in air for dry specimens; (B) at elevated temperature in air for dry specimens; and (C) at room temperature in air for water saturated specimens.

---

* Duco Cement, Devcon Corporation, Danvers Mass.
** Commerical dry wall (gypsum board) was tested in conjunction with the LBWL product, in order to evaluate whether or not the LBWL product could be used as a replacement for dry wall.

(A) Room Temperature Testing

Using a band saw, all LBWL product bend test specimens were cut from microwave processed billets to final specimen dimensions of 12.0 cm * 1.3 cm * 1.3 cm. All modulus of rupture tests were conducted in three point bend in a commerical testing machine (Instron Engineering Corporation model TTCML M1-6). The operating conditions of the test machine were as follows: (1) crosshead speed: 0.1 cm per minute; (2) chart speed: 5 cm per minute; (3) load of full range: 20 kilograms. The three point bend test apparatus was composed of two supports with a span of 4.5 cm and a "hook" like hollow steel plate (Figure 1). The advantages of this load fixture include (1) a tensile load cell was safely used in the test machine instead of a load compression cell* and (2) the load fixture could be placed inside a resistance-heating furnace (Lingberg, Watertown, Wisconsin) in order to assemble an elevated temperature test apparatus (Figure 2). If the specimen broke at mid-span (or the distance from mid-span to fracture surface was less than 1 cm), the test was considered to be a valid bend test and the datum was recorded. If the specimen broke more than 1 cm outside the midspan point, the test was considered to be invalid and the strength datum was not recorded. After rupture, the width,

---

* A compression load cell may be easily damaged by misalignment of the specimen or the load train. A tensile load cell is generally not so easily damaged.

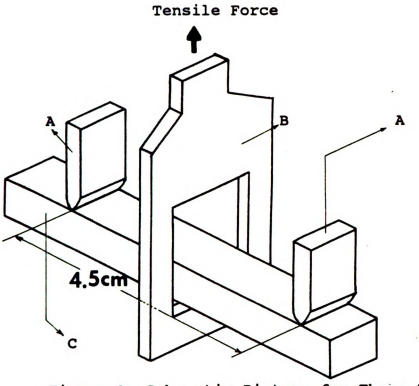

A: Supports with a span of 4.5 cm

B: "hook" like hollow steel plate

C: Specimen

Figure 1. Schematic Picture for Three Point Bend Test

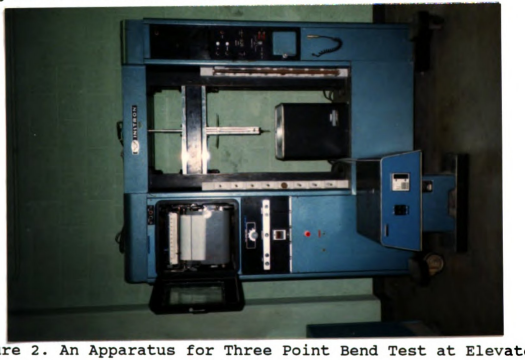

Figure 2. An Apparatus for Three Point Bend Test at Elevated Temperature. A: Universal testing machine. B: Resistance-Heating Furnace. C: Three point bend test fixture.

B, and the depth, D, of the fracture section was measured using a metric dial caliper. The modulus of rupture, the fracture strength of a material under a bending load, is given by

$$MOR = (3 * P * L) / (2 * B * D) \quad (2)$$

MOR = modulus of rupture (MPa)

P = bending load (newton)

L = span between supports (mm)

B = width of the specimen (mm)

D = depth of the specimen (mm)

For each of the seven LBWL compositions listed in Table 4, the value of MOR was obtained from a minimum of 10 specimens.

(B) Elevated Temperature Testing

Besides room temperature tests, the strength of the LBWL product was tested at 200 degrees Celsius and 400 degrees Celsius in air. In the elevated temperature test, specimens of LBWL product of the same dimensions as the room temperature specimens were placed in the test apparatus for 20 minutes before testing in order to allow the specimens to approach thermal equilibrium.

(C) Room Temperature Testing on Water Saturated Specimens

To understand the hydration resistance of LBWL product,

specimens were placed in a 1000 c.c. beaker and soaked in tap water for 2 hours at room temperature and at about 98 degrees Celsius respectively. For the 98 degrees Celsius testing, the water temperature was maintained by a heater placed under the beaker. The soaked specimens were tested using the three point bend test.

(4) Examination of LBWL Product Reheated at Elevated Temperature

In the production of abrasive wheels using aluminosilicate grains and a water glass binder, it has been observed that the wheels can be made more water-resistant, though rather brittle, by firing between 850 degrees Celsius and 1100 degrees Celsius [2]. In order to ascertain whether heating at such temperatures would affect the resistance of LBWL product to water attack, specimens of LBWL product with dimensions of 12 cm * 1.3 cm * 1.3 cm were reheated in air in a resistance-heating furnace. The operating conditions are indicated in Table 5.

The specimens reheated at 800 degrees Celsius were soaked in tap water at about 98 degrees Celsius for 2 hours. Then the strength of the soaked and the unsoaked specimens was determined by means of the three point bend test to understand the extent of water resistance.

After being reheated, the specimens were ground into a powder with a porcelain mortar and pestle. Then each specimen was analyzed by x-ray diffraction. The operating

condition for the x-ray machine was the same as that used for the fly ash.

Table 5. Time Schedule of LBWL Product Specimens* Reheated in Resistance-heating Furnace

Temperature (degrees C.)	Heating duration (hours)
800	16
1000	10
1150	4

* Only the specimens of composition 1, 2, and 3 were reheated and tested.

(5) Compression Test

The specimens were cut into rectangular blocks (3 cm * 1.3 cm * 1.3 cm, approximately) using a band saw. Then they were ground down with a rotating belt sander to smooth and flatten the surfaces. To ensure the flatness of the two end surfaces intended to receive the load from the testing machine, a parallel press was used. (The press has a pair of parallel and face-to-face stages). First, the specimen was placed on the lower press stage and then the upper stage was manually brought down on top of the specimen. If there was no gap between the specimen and the surface of the upper stage, the specimen was judged to be flat enough to be used for the compression test. If the surface was not sufficiently

flat, the specimen was ground again until it reached the desired flatness. The compression tests were done using a Tinius Olson Hydraulic Testing machine. The operating condition was (A) scale of load speed: 10 ; and (B) load cell: "low" range. The cold crushing strength was calculated by:

$$S = W / A \qquad (3)$$

S = cold crushing strength (MPa)

M = total maximum load indicated by testing machine

A = average of the gross areas of the top and button of the specimen (mm)

For each of the seven LBWL compositions and the dry wall, the average value of cold crushing strength was obtained from a minimum of 10 specimens.

(6) Measurement of Thermal Conductivity

The thermal conductivities of LBWL products and the dry wall were determined by the hot-wire method described below. Isolated box: An isolated box, with inner dimensions of 6 cm * 15 cm * 15 cm, was made out of alumina silicate fiber board where the thickness of the fiber board itself was 1 cm. The purpose of the box was to improve the stable heat flow in the specimen. The specimen was tested in the box.
Furnace: In the elevated temperature testing, a resistance-heating furnace, with inner dimension 13.5 cm * 19 cm * 42

cm, was used.

Measuring system: A schematic diagram showing the relationship of all components in this system is shown in Figure 3. A DC power supply with output current 0 - 8 A was used. An iron wire and a constantan wire, both 0.15 mm in diameter and 50 mm in length, were welded together with a spot welder to make a J type thermocouple. An electronic ice point (model: MCJ OMEGA) was used to establish a reference temperature for the thermocouple. The voltage of the thermocouple was recorded with a strip chart recorder (model: RD - 145 OMEGA). The current and voltage of the nickel chromium alloy hot wire, 128 mm in length and 0.4 mm in diameter, was measured using a multimeter (John Fluke MFG. Co., Inc).

Test sample assemebly: For each thermal conductivity measurement, two LBWL product specimens were cut to the dimensions of 12.5 cm * 12.5 cm * 2.5 cm. The dry wall thermal conductivity test specimen had dimensions 12.5 cm * 12.5 cm * 1.2 cm. As was the case for the strength testing, the paper coating of the dry wall was removed before the thermal conductivity testing. The specimen surfaces were made sufficiently flat to sandwich the wires and insure that good thermal contact was made. Grooves for the hot wire and for the thermocouple wire were cut into the specimen with a knife. The groove depth was maintained at approximately 0.5 to 1.0 mm and the groove width was about 0.5 mm, where the groove dimensions were estimated visually. Figure 4 shows

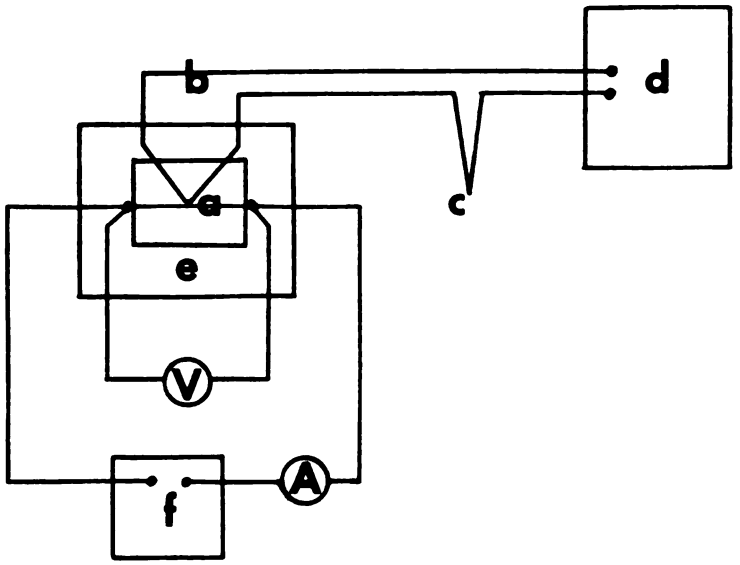

a : Hot wire

b : Thermocouple

c : Ice point

d : Recorder

e : Isolated box

f : DC powder supply

Figure 3. Diagram of Measuring System for Thermal Conductivity.

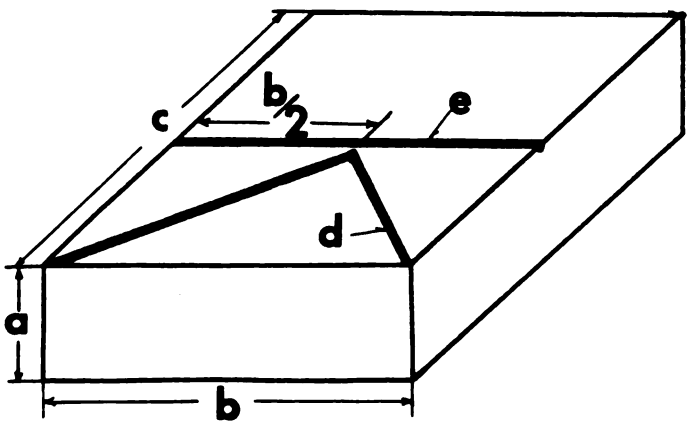

a : 2.5 cm

b : 12.5 cm

c : 12.5 cm

d : Thermocouple groove

e : Hot wire groove

Figure 4. Specimen Size and Location of Groove for Thermal Conductivity Measurement

the size of specimen and the location of the grooves. Before placement into the isolated box, the sample assembly was dried in air at 110 degrees for a minimum of 16 hours.

During the measurement, the current and voltage of the hot wire were measured continuously in order to estimate average values. The thermocouple voltage was recorded on a strip chart recorder at the end of 2 minutes heating of the hot wire. From the chart of voltage versus time, temperature rise versus the logarithm of elapsed time was plotted manually and an s-shaped curve was obtained. The slope of the linear portion of the curve is valid for the conductivity value. The thermal conductivity of the specimen was calculated according to the equation below [3]:

$$K = \frac{Q * Ln\ (t1 / t2)}{(T1 - T2) * 4 * 3.14159} \qquad (4)$$

where: $Q = I * V / L$

Q = heat input per unit length of hot wire (watt / meter).

I, V = current and voltage of hot wire respectively

L = length of hot wire (meter).

t1 and t2 = time elapsed for the linear portion of temperature versus the logarithm of time curve (where time is measured in minutes).

T1 and T2 = temperature of the hot wire at times t1 and t2 respectively (degree C).

(7) Measurement of Thermal Expansion

In the refractories field, thermal expansion is important for thermal shock and thermal spalling investigations. For further study of thermal shock, the thermal expansion coefficient of LBWL products was measured using the Thermomechanical-Analyzer (TMA) (Du Pont Company, Wilmington, DE).

Using a band saw, LBWL product thermal expansion specimens were cut from microwave processed billets to final specimen dimensions of 2 cm * 0.5 cm * 0.5 cm. Then the specimens were heated in air in a resistance-heating furnace to insure their stability while being tested in the TMA. The "stabilization" thermal anneal was carried out in the following way. The microwave processed specimen was placed in air in a resistance heated electric furnace, where initially both the specimen and the furnace were at room temperature. The furnace was then turned on and the temperature control was set to 250 degrees Celsius. After two hours at the 250 degree Celsius setting, the temperature controller was set to 500 degrees Celsius for an additional two hours. The furnace was then turned off for 2 days and allowed to cool freely to reach room temperature. The specimens were then removed from the furnace.

The thermal expansion moduli of the Dupont TMA was operated with the thermal expansion probe. The standard weight on the TMA weight tray was 5 grams. The heating rate for all thermal expansion specimens was 5 degrees per minute

from room temperature to a maximum temperature of 500 degrees Celsius.

(8) Evaluation of Thermal Shock

Thermal shock is caused by thermal stresses in materials. The thermal shock resistance parameter, which is a material resistance factor for thermal stresses, can be derived from the fracture stress necessary to initiate or propagate cracks [4-7]. The resistance of the LBWL products to thermal shock damage was evaluated by three point bend fracture testing on thermally shocked specimens.

The experimental procedure for thermal shock testing was as follows. LBWL product thermal shock specimens were cut into rectanglar blocks of dimension 12.0 cm * 1.3 cm * 1.3 cm, using a band saw. These specimens were set in a cool resistance-heating furnace, and then the furnace was turned on. The heating conditions are indicated in Table 6. The specimens were removed rapidly from the furnace and quenched in room temperature air. Since the LBWL products do not have good resistance to water attack, the specimens were quenched in air instead of immersing in a water bath.

After the specimens cooled to room temperature, the fracture strength of the specimens was measured in three point bend. The thermal shock resistance parameter was calculated by:

$$R = \frac{E}{S * S * (1 - U)} \qquad (5)$$

R = thermal shock resistance parameter

S = fracture stress

U = Poisson's ratio

E = Young's modulus

Table 6. Thermal Shock Conditions for LBWL Product Specimens Heated in Resistance-Heating Furnace

Temperature (degrees C.)	Heating duration (hours)
300	1
500	1
550	1
600	1
630	1
650	1
700	1
750	1

(9) Measurement of Young's Modulus and Acoustic Damping Capacity

The dynamic resonance method is a powerful technique for measuring Young's modulus and internal friction [8,9]. The resonance method is based on a standing-wave phenomenon. When a specimen undergoes a certain longitudinal, flexural, or torsional vibration which forms a mechanical standing-wave in the specimen, the amplitude of the vibration in the

specimen will reach a maximum value. The Young's modulus, E, is proportional to the square of the flexural resonant frequency, while the shear modulus is proportional to the square of the torsional resonant frequency. The internal friction, which is a measure of the mechanical energy dampening character of a specimen, may be calculated using, for example, the Full Width at Half Maximum (FWHM) of the vibrational amplitude versus frequency curve. Methods for calculating both the elastic moduli and the internal friction will be discussed later in this section. This section describes the procedures for resonant frequency measurement and the methods to calculate the Young's modulus and internal friction of the LBWL products.

The measuring system consists of a driving circuit, a pickup circuit, and a specimen support. A schematic diagram showing the relationship of all components in this system is shown in Figure 5. The variable-frequency synthesizer (3325A Synthesizer / Function Generator made by Hewlett-Packard) served as the signal source. This sinusoidal electrical signal was converted into a mechanical vibration via a high power piezoelectric driver transducer (model # 62-1 made by Astatic Corp., Conneaut, Ohio). The mechanical vibration was passed along the support thread through the specimen to another support thread, which was connected to the pick-up transducer. The mechanical vibrations were then converted to an electric signal which was amplified, filtered (4302 Dual 24DB/Octave Filter-Amplifier made by Ithaco), and passed

through a voltmeter (8050A Digital Multimeter made by Fluke), and Oscilloscope (V-100A 100MHz Oscilloscope made by Hitachi).

LBWL product specimens were cut and ground from prismatic bars of dimension 9 cm * 3 cm * 0.7 cm. Cotton support threads were attached to the specimen at 0.5 cm from each end diagonal (Figure 6). The threads to the driver and the pickup transducers were connected as described above.

During the measurement, the oscillator frequency was manually varied from 800 to 7000 Hz in order to find all of the standing-wave vibrations forming in the specimen. If a sharp and maximum amplitude of the vibration appeared on the oscilloscope and digital voltmeter, the frequency was recorded.

To calculate the Young's modulus, one must know exactly the type and mode of the vibration of the specimen. A prismatic bar can be excited in a variety of vibrational modes, including the fundamental flexural frequency, the fundamental torsional frequency, and overtones of each of these frequencies. Thus if one identifies a resonant frequency, one must determine which particular mechanical vibrational mode is being excited before a determination of elastic modulus can be made. The vibrational mode can be identified by locating the position of the vibrational nodes and antinodes along the specimen in which a standing-wave vibration forms. The positions of the nodal and antinodal lines on a prismatic bar-shaped specimen vibrating at a mechanical resonance may be determined by mechanically

Figure 13.

(C)

Figure 5. Outline of Apparatus for Measuring the Elastic Modulus (Dynamic Resonance Method).

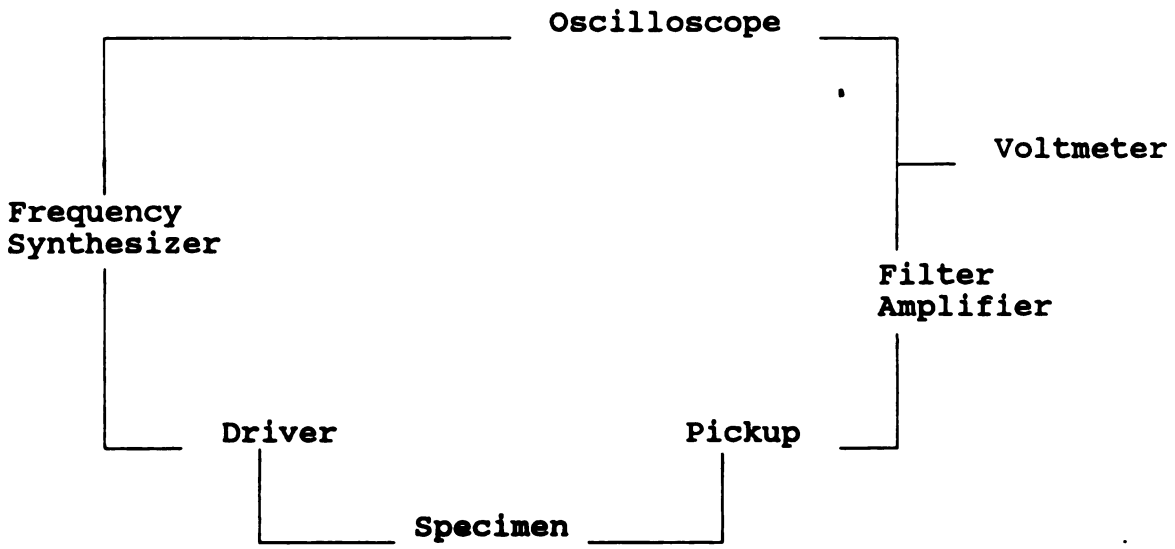

Figure 6. Illustration of Method of Coupling Acoustic Energy

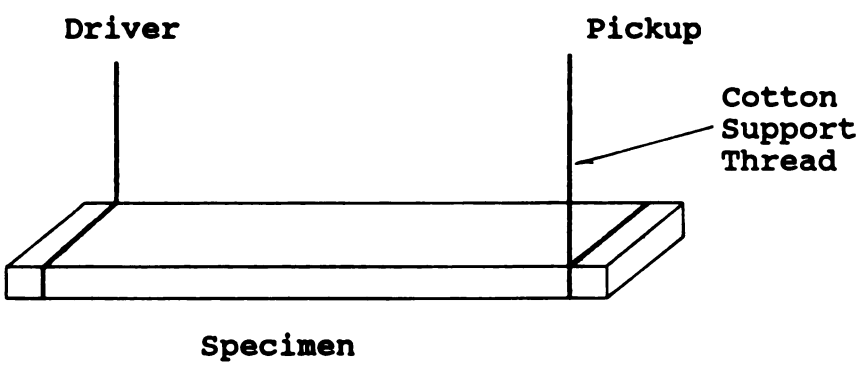

"probing the bar" [8]. In this study, the nodal and antinodal positions were probed using a sewing needle, balanced at various locations along the length of the resonating bar. When the needle is set on a nodal line, the amplitude of resonant frequency will change very little. If the needle is positioned away from a nodal line, then the needle will dampened the mechanical vibrations in the specimen and the vibrational amplitude will be reduced. Anderson [8] indicates the position of the nodes as a fraction of the length of the specimen (Table 7).

After the indentification of the resonant frequency, the Young's modulus, shear modulus, and Possion's ratio can be calculated as follows*:

$$E = 0.94642 * \frac{P * F * T * L^4}{D^2} \qquad (6)$$

E = Young's modulus of elasticity

F = fundamental flexural frequency

L = length of the specimen

P = mass density of the material

D = cross sectional dimension in the direction (or plane) of vibration

T = correction factor

---

* The elastic modulus calculations were performed using a computer program derived by professor Eldon Case, Department of Metallurgy, Mechanics, and Materials Science, Michigan State University.

Table 7. Position of the Vibrational Nodes of a Prismatic Specimen. The Nodal Positions are Expressed as a Fraction of the Length of the Specimen

Mode of vibration	Flexural vibration	Torsional vibration
Fundamental	0.224	0.500
	0.776	
First overtone	0.132	0.250
	0.500	0.750
	0.868	

The correction factor T is approximated by

$$T = 1 + 6.58\,(1 + 0.0752\,U + 0.8109\,U^2)\,(D/L)^2 - 0.868\,(D/L)^4 - \frac{8.34\,(1 + 0.2023\,U + 2.173\,U^2)\,(D/L)^4}{1 + 6.338\,(1 + 0.1408\,U + 1.53\,U^2)\,(D/L)^2}$$

U = Poisson's ratio

The equation which relates the torsional resonance frequency with the shear modulus is

$$G = P\,(2L * F / N)^2 * R$$

G = shear modulus

N = an integer which is unity for the fundamental mode,

two for the first overtone, etc.

F = torsional reasonance frequency

R = shape factor which depends on the shape of the specimen

L = specimen length

P = mass density of the material

For prismatic specimens of rectangular cross section, R can be approximated by an equation as follows:

$$R = \frac{1 + (b / a)^2}{4 - 2.521\,(a/b)\left[(1 - 1.991)/(e^{b/a} + 1)\right]}\left(1 + \frac{0.0085\,N^2 b^2}{L^2}\right) - 0.06\,(Nb / L)^{1.5}\,(b/a - 1)^2 \qquad (8)$$

a = thickness of specimen

b = width of specimen

Poisson's ratio of a homogeneous isotropic body is expressed by:

$$U = E / 2G - 1 \qquad (9)$$

Internal friction of solids is one of the important characteristics directly related to the acoustic damping properties of materials. In addition to measuring Young's modulus, the dynamic resonance method also can be used as a forced vibration method to measure internal friction [8,9]. The LBWL product's internal friction can be calculated by

$$Q = 0.5773 \frac{\blacktriangle F}{F}$$

where F = the resonance frequency of the specimen, for example, the flexural or the torsional vibrational frequency of the specimen.

$\blacktriangle$ F = the Full Width at Half Maximum (FWHM) for the amplitude versus frequency peak that occurs at a mechanical resonance. If the resonant frequency occurs at a frequency Fo with amplitude Ao, then the FWHM value corresponds to the difference F2 - F1, where F2 and F1 are the frequencies on the shoulders of the resonance peak having amplitude Ao/2.

In this study, the fundamental flexural frequency was chosen as the resonance frequency to be used in the internal friction measurements. For the LBWL product tested, the flexural resonant frequencies ranged from 1200 Hz to 2500 Hz, which includes the frequency range of common environmental noises found in commercial buildings and dwellings. The range of human hearing is about 20 Hz to 20 KHz, although most human speech occurs in a frequency band from about 500 Hz to a few kilohertz. Thus, the range of resonant frequencies used in the internal friction measurements corresponds to typical noise frequencies found in buildings. Therefore the internal friction (mechanical energy dampening) is quite appropriate to assess the sound dampening behavior of potential building materials such as the LBWL product.

RESULTS AND DISCUSSION

Before discussing the mechanical and thermal testing of the LBWL product, the analysis of the raw materials that comprise the LBWL product will be considered. Sludge, fly ash, and water glass are the main ingredients in LBWL product. To investigate the characteristics of LBWL product, the ingredients of the LBWL product were analyzed by such techniques as x-ray diffraction, SEM, and optical microscopy. The mechanical and thermal properties of the LBWL product were then examined.

I. Analysis of Sludge

The x-ray diffraction traces of sludge powder showed some predominant and many low intensity peaks, listed in Table 8. The peaks are believed to be representative of the crystalline phases of calcium carbonate and magnesium hydroxide. A comparison of diffraction traces of pure calcium carbonate and sludge powder indicates that the main component of sludge is the calcium carbonate (Appendix A). The diffraction traces of heated sludge powder indicates that the sludge undergoes the following chemical reaction:

$$CaCO_3 + Mg(OH)_2 \quad (\text{sludge}) \xrightarrow{\text{at 400 C for 3 hours}} CaCO_3 + MgO$$

$$CaCO_3 + Mg(OH)_2 \quad (\text{sludge}) \xrightarrow{\text{at 800 C for 3 hours}} CaO + MgO$$

Magnesium hydroxide decomposes at 350 degrees Celsius and calcium carbonate be can calcined at about 825 degrees [10]. Since LBWL product was heated by microwaving, the influence of temperature on sludge deserved consideration.

Table 8. The Diffraction Data of Sludge

Sludge		Sludge heated at 400 C		Sludge heated at 800 C		Pure $CaCO_3$		$CaCO_3$ heated at 800 C	
d(A)	I/I.	d(A)	I/I.	d(A)	I/I.	d(A)	I/I.	d(A)	I/I.
4.79a	5	3.85	3	2.76	31	3.85	8	2.77	32
3.88	8	3.03	100	2.39	100	3.04	100	2.40	100
3.05	100	2.48	15	2.10c	20	2.84	3	1.70	45
2.50	13	2.27	23	1.69	52	2.49	14		
2.37a	10	2.09b	23			2.28	22		
2.29	20	1.91	25			2.09	19		
2.09	18	1.87	26			1.90	24		
1.90	24					1.87	24		
1.87	24					1.62	5		
1.80a	5					1.60	12		
1.57a	4								

* a. Magnesium hydroxide. b. Diffraction peaks for calcium carbonate and magnesium hydroxide. c. Magnesium oxide.

Table 9. The Diffraction Data of Fly Ash

Fly ash		Magnetic particles		Fly ash reheated at 1200 degrees		Pure mullite	
d(A)	I/I.	d(A)	I/I.	d(A)	I/I.	d(A)	I/I.
5.4	23	2.98m	37	5.4	41	5.4	34
4.28q	26	2.71h	41	3.41	100	3.41	100
3.40	53	2.54m	100	2.89	24	2.89	16
3.34q	100	2.22	16	2.70	48	2.70	36
2.89	11	2.11m	24	2.55	56	2.55	39
2.70	31	1.85	22	2.43	22	2.43	12
2.55	34	1.70h	26	2.30	24	2.29	18
2.30	23			2.21	67	2.21	52
2.21	41			2.12	21	2.12	22
2.12	19			1.85	16	1.90	6
1.82q	14			1.72	16	1.84	9
				1.70	21	1.71	6
						1.69	14

q. Quartz. m. Magnetite. h. Hematite.

II. Analysis of Fly Ash

(1) X-ray Diffraction Analysis

According to the x-ray diffraction analysis in Table 9, the major crystallographic phases present in the LBWL fly ash are mullite ($Al_6Si_2O_{13}$) and Quartz (SiO_2). In the magnetically separated fractions of the fly ash, x-ray diffraction indicates the presence of minor concentrations of iron oxides such as hematite (Fe_2O_3) and magnetite (Fe_3O_4) Moreover, a broad "hump" extending between about 15-35 degrees (2θ) in the diffraction pattern indicates the presence of a glassy phase in the fly ash.

In addition to the compounds mentioned above, some minor amounts of crystalline calcium ferrite, ferrite spinel, mica, feldspar, bredigite, nepheline, hydrite, periclase, merwinite, rutile, barite, nepheline, lime, calcium oxide, and magnesium oxide have been observed in other fly ash specimens by other researchers [11-15]. However, none of these minor components were identified in the Lansing Board of Water and Light fly ash.

(2) Microscopy of Fly Ash Powder

SEM and reflected light microscopy examination of fly ash powders showed that the majority of particles were spheres approximately 5-40 microns in diameter (Figure 7). The surfaces of the fly ash particles were rather smooth, but

(A)

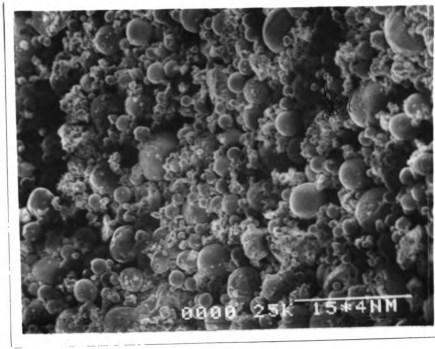

(B)

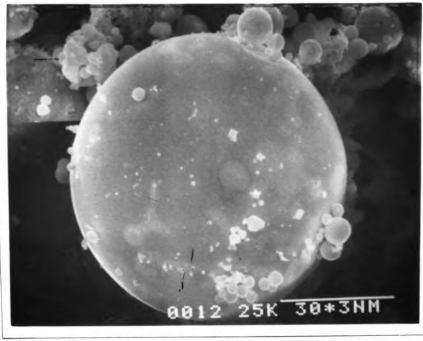

Figure 7. Scanning Electron Micrographs of (A) As-received Fly Ash at 200X Magnification, (B) Spherical Fly Ash at 1000X Magnification, (C) Rough and Pebbly Fly Ash at 1000X Magnification

Figure 7

C :

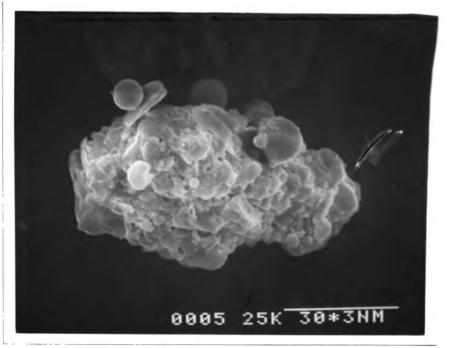

in some ashes they tended to be rough and pebbly. Additionally, hollow spheres with or without small incorporated fly ash spheres were found on occasion. Empty hollow spheres are called cenospheres (Figure 8). Those hollow spheres that contain included spheres are called plerospheres [11,16-19]. Both types of spheres are always observed in SEM since the shells may be incomplete or broken in spots. Completely unbroken hollow spheres can not be recognized as such.

When fly ash powder was treated by the organic liquid (60 percent methyl ethyl ketone, peroxide in dimethyl phthalate), some irregularly shaped lumps with diameters generally greater than 300 microns were extracted from the fly ash powder. When the fly ash was reheated to 800 degrees Celsius, the lumps disappeared. These particles are probably unburnt coal. As viewed by reflected light microscopy, they appear white in some sections because of their high reflectivity. In other locations in the fly ash specimen the original structure of the coal may be partially retained. Pieces of mineral matter transformed into spherical particles are sometimes evident. A SEM photograph of a coal particle with some spherical inclusions of mineral matter in cell voids is shown in Figure 9.

Iron oxide particulates are easily identified in microscopic studies by taking advantage of their magnetic properties. The black magnetic particles appear as spheres when observed in a reflected light microscope and in the SEM (Figure 10a). A dendritic structure was revealed after the

particle was etched by HF + HCl solution (Figure 8b). The dendritic habit is considered indicative of rapid crystallization [11]. The black magnetic particles reheated at 800 degrees Celsius for 5 hours had no color change. The crystalline magnetite and hematite may have developed as inclusions in the glassy phase material (Figure 10c), then a thin glass would cover the magnetic particles so that magnetite would not oxidize to yellow-red hematite.

(3) Fly Ash Reheated From 300 to 1000 Degrees Celsius

The fly ash reheated at 300, 500, 800, and 1000 degrees Celsius showed no change in x-ray diffraction pattern. Thus the mineralogical composition of fly ash did not change during the reheating process, for temperatures up to 1000 degrees Celsius. However, the color of fly ash reheated at 800 and 1000 degrees Celsius turned from gray to orange-red and the weight of the fly ash decreased by 3.8 weight percent. The burn-out of the residual coal and volatile material in fly ash probably accounts for most of the weight loss.

(4) Fly Ash Reheated at 1200 Degrees Celsius

Some crystallographic phase changes did occur for fly ash reheated at 1200 degrees Celsius. The x-ray diffraction data indicated that mullite was still a major crystalline

(A)

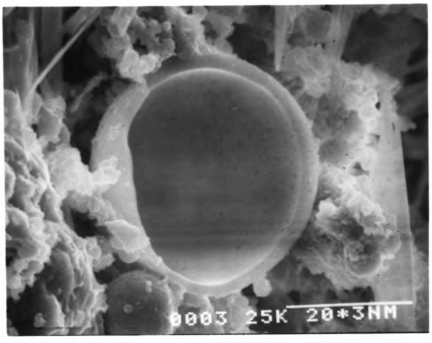

(B)

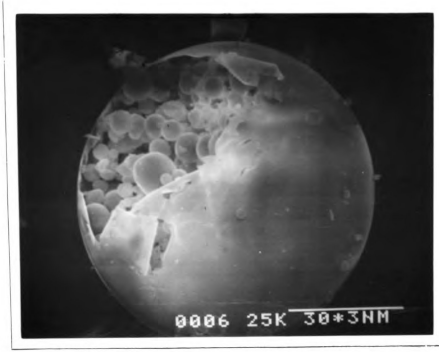

Figure 8. Scanning Electron Micrographs of (A) Cenospherical Fly Ash at 1500X Magnification and (B) Plerospherical Fly Ash at 1000X Magnification

(A)

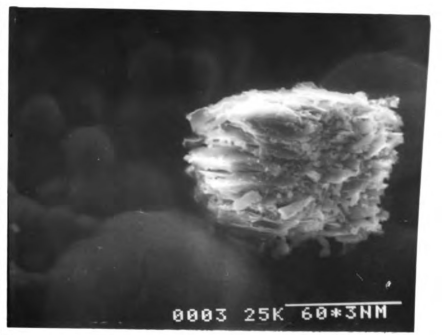

(B)

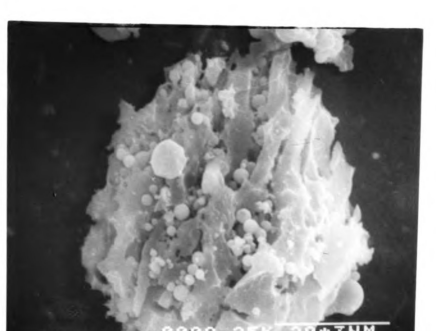

Figure 9. Scanning Electron Micrographs of Coal Particle in Fly Ash (A) at 500X and (B) at 1500X Magnification

(A)

(B)

Figure 10. Scanning Electron Micrographs of (A) Magnetic Particle Without Chemical Etching (1500X Magnification), (B) and (C) Magnetic Particle After HF + HCl Etching for 15 Minutes (2000X Magnification)

Figure 10.

(C)

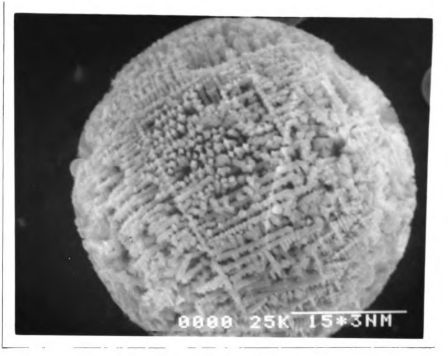

component (as it was in specimens reheated at lower temperatures), but quartz diminished considerably (see Table 9). In addition, the fly ash reheated at 1200 degrees Celsius showed some sharpening of x-ray diffraction lines, which were sharper than those in other kinds of fly ash. This was indicative of a coarsening of the mean particle size of the fly ash particles due to thermally induced diffusion. (Powders with mean particle sizes less than about 20 microns show a characteristic broadening of their x-ray diffraction peaks.) Another substantial indication of appreciable diffusive mass transfer was that the fly ash placed loosely in an alumina crucible sintered and shrank to a very hard aggregate. A third indication of appreciable mass transfer was that upon heating at 1200 degrees Celsius, the morphology of the fly ash changed from spheres to plate-like particles (Figure 11). Fly ash particles reheated at 1000 degrees Celsius or lower temperatures did not show this shape change.

For most ceramic powders, if a loose powder begins to sinter noticeably at temperature T1, then a powder compact* will sinter at temperature T2, where T2, the sintering temperature for the powder compact, is considerably lower by perhaps 100 degrees Celsius or more than T1, the sintering temperature for the loose powders. Thus the fly ash may begin to sinter appreciably at temperatures as low as 1100 degrees Celsius if a powder compact (pellet) is first formed from the fly ash powders.

---

* For example, a pellet formed by uniaxial pressing of the initial powders.

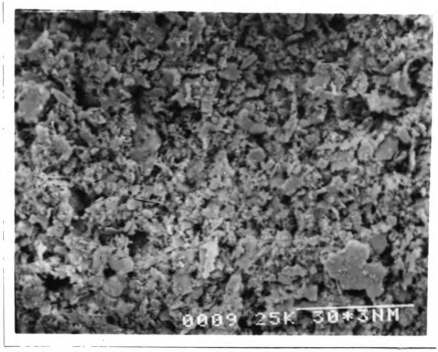

Figure 11. Scanning Electron Micrograph of Fly Ash Reheated at 1200 Degrees Celsius (1000X Magnification)

(5) Fly Ash Reacted with Water Glass and Phosphoric Acid

Since water glass was used as a binder in LBWL product, the reaction of water glass with fly ash was studied. After soaking fly ash powder in a water glass solution for 14 hours, SEM and optical microscope examination showed no evidence that the particles of fly ash had changed. It is believed that the fly ash could be regarded mainly as a filler in the LBWL product instead of the reactant.

Water glass can react with acids such as phosphoric acid to form a silica gel that is insoluble in water [10,20]. This insoluble reaction product is expected to improve the resistance of LBWL product to water attack. Consequently, the reaction of phosphoric acid with fly ash and water glass is of interest. The reaction between water glass and phosphoric acid will be discussed in the section of this report entitled "Water Glass and Production of the LBWL product."

If phosphoric acid is added to the LBWL product, then in addition to the reactions between the fly ash and the water glass, one must consider the reactions between the fly ash and phosphoric acid. Soaking fly ash powders in phosphoric acid at room temperature for 14 hours had at least two effects. The first effect of the phosphoric acid upon the fly ash powders was that the fraction of magnetic particles per unit volume was decreased, presumably due to the solubility of the magnetic particles in phosphoric acid. A second, and potentially very important effect of the 14

hour, room temperature soak in phosphoric acid was that the surface appearance of individual fly ash particles changed as a result of this treatment. For example, SEM microscopy (Figure 12) revealed that the surface of fly ash particles were roughened and pitted by the acid treatment. The removal of mass on the surface of fly ash particles likely creates fresh powder surfaces. Fresh powder surfaces can significantly enhance the sinterability of a ceramic powder. Thus if one intended to sinter a fly ash powder compact, a treatment in acid may aid the sinterability of the powder. Such a sintering experiment (using acid treated fly ash powders) was not attempted in this study since for the LBWL product, the microwave processing is essentially a "cold bonding" process in which the water glass acts as the binding phase in the material. However, if the fly ash were to be sintered at elevated temperatures, this study shows that acid treatment does alter powder surfaces in a way that is potentially very beneficial to sintering.

(6) Summary of the Analysis of Fly Ash Powder, Water Glass, and Other LBWL Product Reagents

In order to make the best use of fly ash in the LBWL product, the investigations above attempted to understand the properties of fly ash, the influence of temperature on fly ash, and the possible chemical reactions between water glass, phosphoric acid, and fly ash. To the extent that this was

Figure 12. Scanning Electron Micrograph of Fly Ash after Phosphoric Acid Etching for 14 Hours (1000X Magnification)

possible, the following conclusions are made:

(A) The major phases in the Lansing Board of Water and Light fly ash include mullite, quartz, and a glassy phase. Hematite and magnetite are the main minerals in the minor concentration of iron-bearing particles.

(B) Fly ash particles are mostly spherical and approximately 5-40 microns in diameter.

(C) The fly ash received from Board of Water and Light on December 20, 1985 contains approximately 3.8 weight percent of unburned coal.

(D) When fly ash is heated to about 800 degrees Celsius, the remaining coal burns out and the macro color of the fly ash becomes orange-red.

(E) A fly ash compact powder begins to sinter at 1100 degrees Celsius.

(F) Since the temperature of LBWL product in the microwaving process only reaches 220-270 degrees Celsius, the minerals in fly ash are stable during the heating process. Fly ash may be regarded as a filler in LBWL product. The water glass serves as a binder, bonding the fly ash particles together.

III. Water Glass and Production of LBWL Product

(1) Characteristics of Water Glass

In the production of ceramics, binders are sometimes used. These binders are sorted into four catagories [16]:

(A) hydraulic, for example, portland cement.
(B) organic, like coal tar and asphalt.
(C) chemical, such as phosphate bonding.
(D) water glass (sodium silicate, potassium silicate) and minerals.

Water glass is of particular interest in the field of ceramics. It is not only a powerful flux for forming a glass at high temperature [21], but also it is a common bonding medium in the cold-setting process [2,20]. The temperature of a specimen heated in a microwave for ten minutes reaches only 220-270 degrees Celsius. Since the fly ash and sludge in the LBWL product are quite stable at these low temperatures, it may be concluded that the LBWL product hardens by a cold-setting process in which the water glass acts as a binder.

There are two types of hardening mechanisms for ceramics in which soluble silicates such as water glass are used [2,20]:

(A) loss of moisture from the silicate solution.
(B) chemical reactions with the silicate to form stable

silica sols or precipitates.

An example of an industrial process in which a cold-setting ceramic hardens primarily by loss of moisture is the production of a grinding wheel [2]. First, aluminosilicate abrasive grains and water glass are mixed together to produce a green body. The green body is then dried in air at temperatures below 100 degrees Celsius. Finally, the wheel is fired at 180-260 degrees Celsius until it has throughly hardened. The aluminosilicate abrasive grains act as a filler substance with water glass acting as a bond phase.

Cold-setting ceramics made up of water glass are easily attacked by water [2,20-22]. In order to achieve a more water resistant product using low processing temperatures, one could use a chemical reaction with water glass to improve the water resistance of the LBWL product. A chemical reaction can also affect the speed of set and the strength of the product [2].

Water glass may react with mineral acids and acid salts, soluble compounds of metals which form insoluble silicates, or concentrated solutions of ammonium salts to form sols or gels, depending on the concentrations [10,20,23]. In addition to the reagents mentioned above, water glass also can react with some materials that are insoluble in water. For example, calcium oxide reacts with water glass with visible changes occuring within a few minutes. Zinc oxide [2] and calcium hydroxide [20] react similarly.

(2) Qualitative Pretest of Water Glass

To determine trial compositions for LBWL products and to explore the function of phosphate in LBWL products*, some qualitative mixing pretests were performed in which various reagents were mixed with water glass (the weight ratio of SiO_2 to Na_2O : 3.25). The chemical phenomena observed in the pretests are summarized in Table 10.

$Na_4P\ O_7$, $K_4P\ O_7$, and H_3PO_4 are soluble in water. In the pretest, they reacted almost instantaneously with water glass; a rapid rise in viscosity took place. When additional amounts of the reagents were gradually added, the solution changed from a viscous liquid to a gelatinous bulk, and finally to a system of separated precipitates.

When $CaCO_3$ powder, a slightly soluble salt in water, was added to the water glass solution, no visible change was detected within three hours. The viscosity of water glass also did not change as a result of the calcium carbonate addition.

In contrast to the reaction with calcium carbonate, CaO, MgO, and $Mg(OH)_2$ visibly reacted with water glass, so that the particles weakly aggregated together and the water glass gradually became less viscous. CaO apparently reacted much faster with water glass than MgO and $Mg(OH)_2$ did.

The sludge received from Board of Water and Light did not undergo any obvious reaction during the pretest, such as

---

* $Na_4P_2O_7$ and $K_4P_2O_7$ were used in compositions 1, 2, 3, produced by the Lansing Board of Water and Light.

the formation of sludge powder aggregates. When the sludge was blended into the mixture of water glass and fly ash (the final weight ratio: 52 percent fly ash, 26 percent water glass, 11 percent sludge, 11 percent tap water), to form the LBWL product the sludge reduced the adhesion of the mixture. Undoubtedly, some reactions occured. Morgan [20] indicates that even at concentration levels of 1 percent, soluble salts like magnesium chloride or magnesium sulfate can solidify an entire water glass solution. Minor impurities in sludge could be important reactants to alter the behavior of water glass in the mixture.

(3) Production of LBWL product

A suitable amount of $Na_4P_2O_7$, $K_4P_2O_7$, and H_3PO_4 can promote the workability of the LBWL unfired body because of partial gelation. However, an extra amount of the phosphates decreases the strength of the unfired body.

Stronger specimens can not be produced by adding more water glass since the extra soluble silicate solution accumulates on the specimen's upper surface, forming an airtight cover during microwaving. A large expanding bubble then forms below the specimen's surface. On the other hand, when the unfired body contains more water, the shrinkage is more serious. The outer edge of the unfired body is at a higher temperature in the microwave than the central region of the body; therefore faster solidification of the outer

surface leads to shrinkage and cracking in the central part of the body.

Efficient bonding between particles is not based on the large additions of water glass, but rather on the integrated control of the following factors: (A) the types of bonds; (B) the amount of the binder; (C) the density of the ceramic; (D) the packing density; and (E) the cohesive or adhesive strength of the binder [24-26]. The solidification of water glass on the surface of fly ash particles resulted in a bonding between individual fly ash particles. Consequently, liquid viscosity, water content [27], surface tension, wetting characteristics, mixing time, soaking duration, and the penetration of liquid into porous solids [26] should be considered. In short, high water glass content in compositions 1, 2, and 3 does not seem to be economical. Knowledge of the physical and chemical processes on which LBWL product depends is not yet sufficiently complete to forecast the behavior of LBWL product for an arbitrary combination of ingredients. The study of compositions 4, 5, 6, and 7 included in this study, however, helps in understanding the role of water glass, fly ash, and phosphate additives in the LBWL product.

Table 10. Chemical Phenomena Observed upon Mixing Various Reagents with Water Glass

Reagent	Reaction Rate	Result
Sodium phosphate	fast	gelation
Potassium phosphate	fast	gelation
Phosphoric acid	fast	gelation
Sludge	too slow to detect	
Calcium carbonate	too slow to detect	
Calcium oxide	fast	aggregates formed
Magnesium oxide	slow	aggregates formed
Magnesium hydroxide	very slow	aggregates formed

IV. Analysis of LBWL Product

(1) X-ray Diffraction of LBWL Product

The x-ray diffraction pattern for LBWL product Composition 1 shows major crystalline components of mullite and quartz, very similar to the fly ash alone (Table 11). The addition of amorphous sodium silicate (water glass) does not contribute additional diffraction peaks, but the sodium silicate addition to Composition 1 does significantly enhance the very diffuse "amorphous scattering" background also seen in the fly ash diffraction pattern. Generally speaking, the x-ray diffraction due to amorphous (glassy) phases can be seen as a low amplitude "hump" in the background. X-ray diffraction peaks of the crystalline phases are superimposed upon this amorphous background. In the case of the fly ash, the amorphous "hump" extends over a 2θ range of about 15-35 degrees. However, for composition 1, the amorphous background is considerably more pronounced than in the fly ash, and it extends to higher 2θ angles.

X-ray diffraction patterns for compositions 2 and 3 are very similar to that for composition 1, except that the composition 2 and 3 patterns include peaks resulting from $CaCO_3$ additions, which indicates that a least part of the $CaCO_3$ is retained during the microwave processing of the product. $Mg(OH)_2$ x-ray diffraction peaks are not apparent for composition 2 and 3. A chemical reaction between water glass and $Mg(OH)_2$ also was not detected, probably because the

amounts of the residual $Mg(OH)_2$ and the reaction product are rather small.

Table 11. X-ray Diffraction Data of LBWL Product

Composition 1		Composition 2		Composition 3	
d (A)	I/I.	d (A)	I/I.	d (A)	I/I.
5.4	24	5.4	9	5.4	25
4.28q	17	3.4	29	4.28g	18
3.4	58	3.34q	63	3.4	59
3.34q	100	3.04c	100	3.34q	100
2.7	32	2.7	25	3.04c	54
2.55	32	2.55	22	2.7	32
2.3	12	2.49c	19	2.55	32
2.21	35	2.29q+c	32	2.3q+c	25
2.12	9	2.21	32	2.21	32
1.82q	10	2.10c	20	2.12	8
		1.91c	26	2.10c	12
		1.87c	25	1.91c	18
				1.87c	14

q. Quartz. c. Calcium carbonate

(2) SEM Investigation of LBWL Product

The SEM investigation of fracture surfaces of the LBWL product shows that compositions 1, 2, and 3 are composed of pores and solid matrix (Figure 13). The water glass binder added to the LBWL product in the form of a water solution forms a solid film on the fly ash when water is removed from the product during microwave processing. Presumably because of chemical reactions between the water glass and some ingredients, the viscosity of the binder is decreased. The solid film in composition 1 develops a three-dimensional structure between fly ash particles (Figure 13a). Composition 2 forms a more open, somewhat plate-like structure (Figure 13b). Sludge inclusions in compositions 2 and 3 range in size from a few millimeters in diameter to much smaller, microscopic inclusions. If one touchs the point of a scribe to one of the sludge inclusions, the inclusion easily crumbles and detaches from the matrix material, thus demonstrating the inclusion's lack of mechanical integrity. In short, the sludge (some soluble impurity and $Mg(OH)_2$) reacts with water glass such that the strength of the LBWL products decreases as the fraction of sludge increases. In addition, the unreacted sludge inclusions (mainly $CaCO_3$) weaken the LBWL product by replacing the bonding phases.

(A)

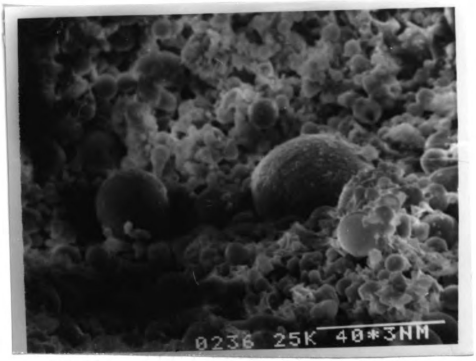

(B)

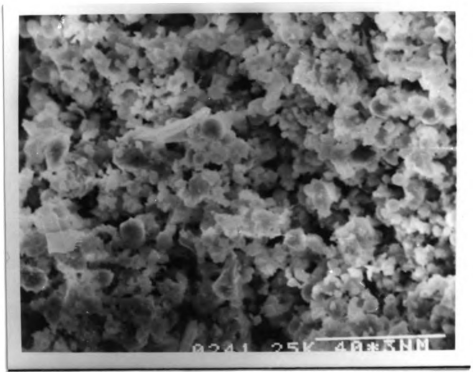

Figure 13. Scanning Electron Micrographs of Fracture Surface of LBWL Product at 750X Magnification

(A) Composition 1. (B) Composition 2. (C) Composition 3.

Figure 13.

(C)

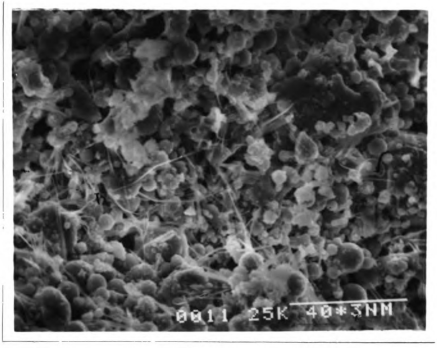

(3) Testing of Mechanical Properties of LBWL Products

The measurement of mechanical strength is a basic procedure in refractory research. The strength of a new material may indicate if the processing techniques are suitable or if the new composition is acceptable. For example, an unsuitable processing technique or composition can result in excessive porosity and weak bonding in the refractory, which would in turn result in a reduction in strength.

Results of the three point bend, compression, density, and water absorption tests are summarized in Table 12. Comparing the data, we may draw the conclusion that:

(A) The flexural strength of LBWL products decreases when they are tested at elevated temperature (Figure 14). However, LBWL products have higher thermal stability than dry wall (gypsum board). The flexural strength of dry wall becomes very low when it is tested at the temperature higher than 200 degrees Celsius.

(B) Sludge decreases the ultimate strength in the three point bend test and the compression test. As more sludge is added, the strength decreases (Figure 15).

(C) Sludge can increase the water-resistance of LBWL products. Figure 16 indicates that composition 6, containing the most sludge, has the least reduction of flexural strength and the highest strength after soaking in water at 98 degrees Celsius for two hours.

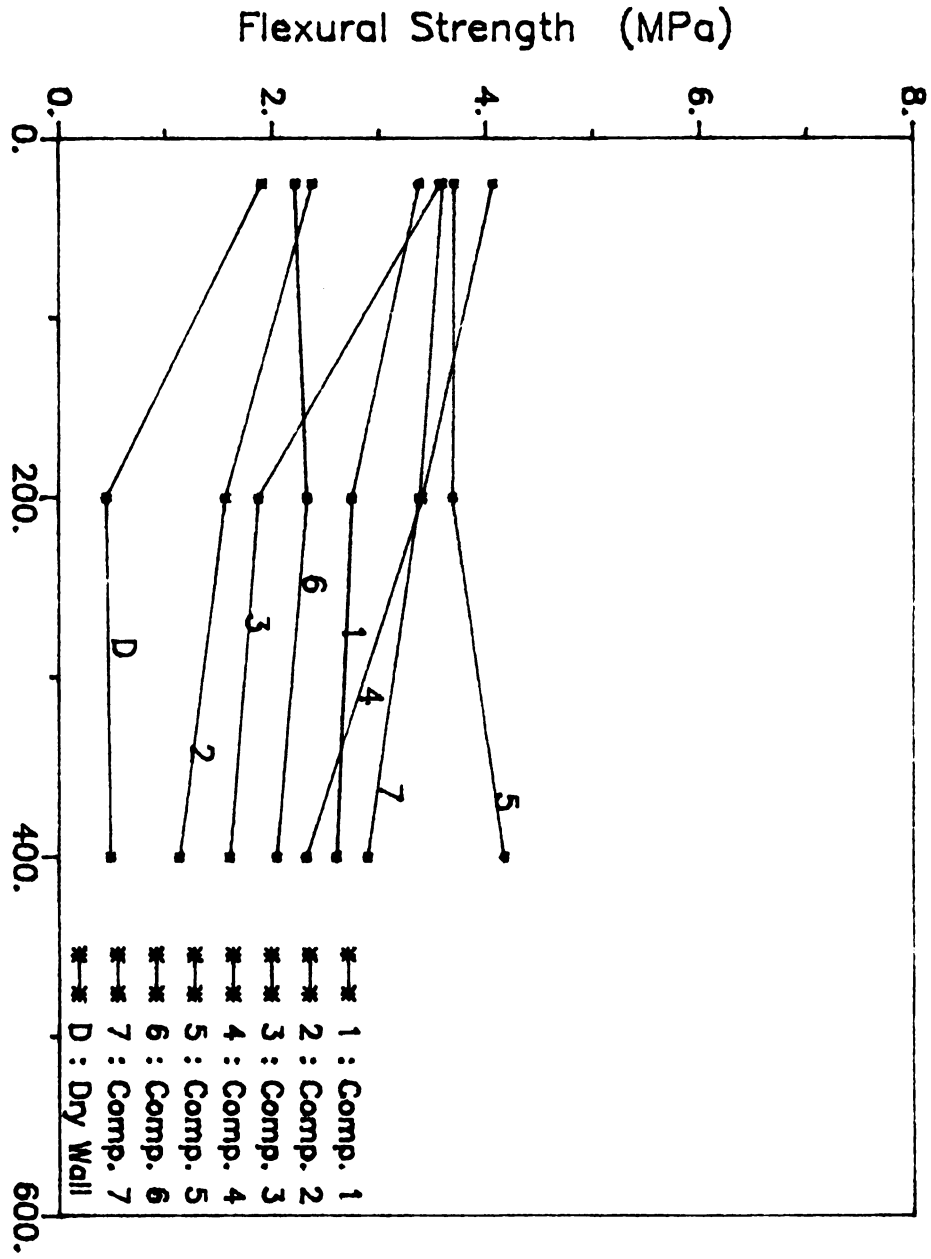

Figure 14 – Flexural Strength of LBWL Product by Means of Three Point Bend Testing

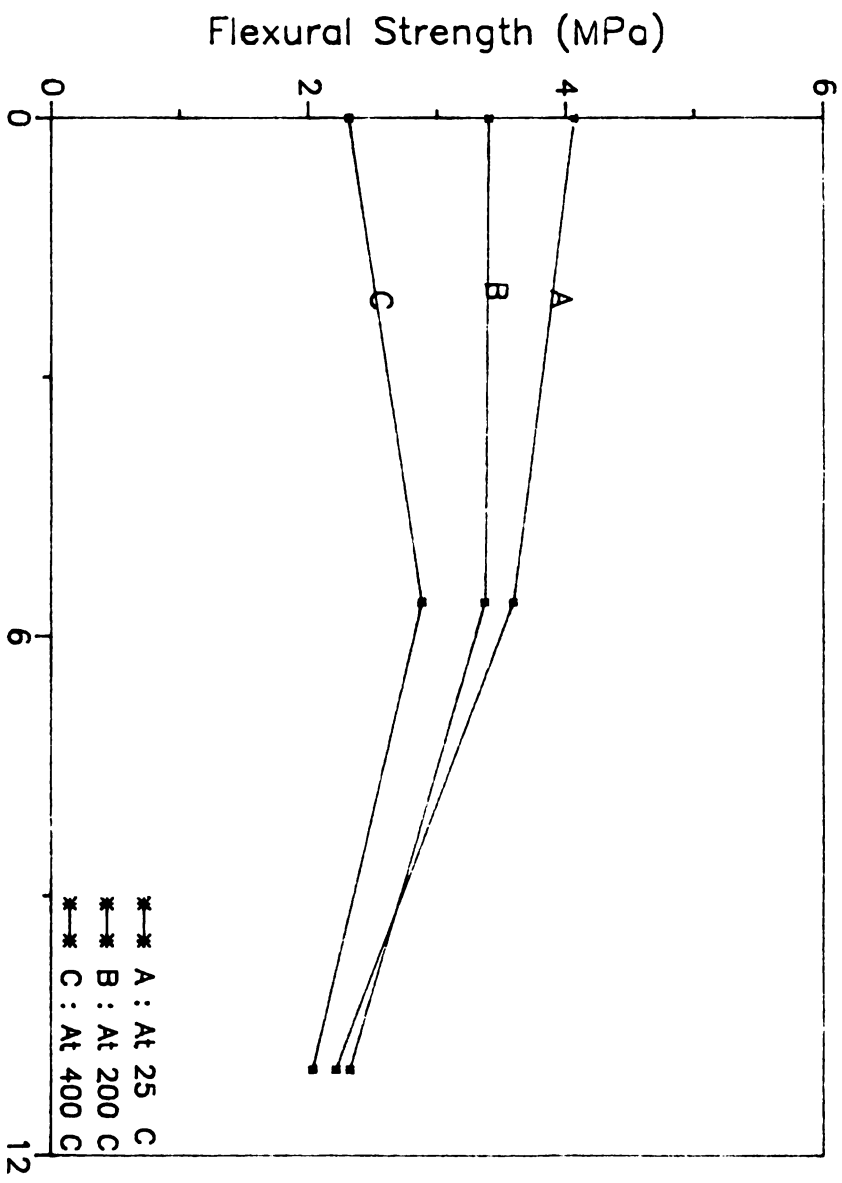

Figure **15** –Influence of Sludge on the Strength of LBWL Product

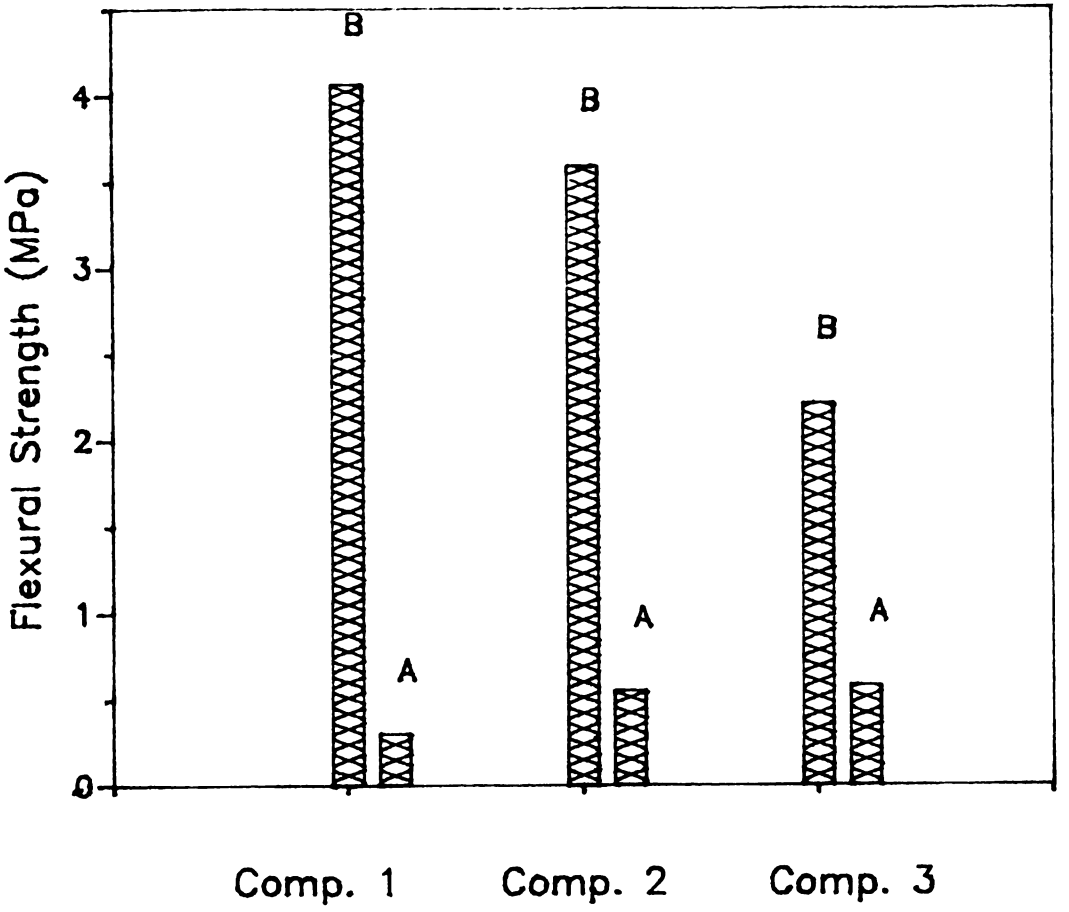

Figure 16 – The Influence of Sludge on Water Resistance. B : The Strength of LBWL Product Before Soaking in Water. A : After Soaking in Water

(D) Phosphate and phosphoric acid, which react with water glass to form a water insoluble silica gel, do not increase the resistance of LBWL products to water attack. Compositions 1 and 5 containing phosphate and phosphoric acid respectively ruptured spontaneously while soaking in water at 98 degrees Celsius for 2 hours (Table 12).

(E) The main function of phosphate in compositions 1, 2, and 3 apparently is to improve the workability of unfired LBWL product, since the addition of small amounts of phosphate to the unfired LBWL product acts to increase the viscosity of water glass.

(F) As shown in Table 12, the mechanical properties of the Lansing Board of Water and Light product exceed those of dry wall (gypsum board) in all of the mechanical tests performed. The only positive result for the gypsum board appears in its mass density rather than in terms of its mechanical properties. The mass density of the dry wall is lower than each of the LBWL products, except composition 1. A low mass density is an obvious advantage in terms of a use as a building material.

The comparison of modulus of rupture among LBWL products and several refractory materials is listed in Table 13.

Table 12. Modulus of Rupture, Compression Strength, Mass Density, and Water Absorption Data for the LBWL Product

Composition	1	2	3	4	5	6	7	dry wall
Modulus of rupture (MPa)								
at 25 C	3.37	2.37	3.57	4.06	3.70	2.21	3.59	1.90
at 200 C	2.74	1.55	1.86	3.40	3.68	2.32	3.37	0.44
at 400 C	2.59	1.12	1.59	2.31	4.16	2.03	2.88	0.48
Modulus of rupture after soaking in water for two hours (MPa)								
at 25 C	1.16	0.72	1.27	3.00	3.13	1.92	3.36	0.37
at 98 C	None*	0.56	0.75	0.30	None*	0.58	0.55	0.31
Cold compression strength (MPa)	3.61	4.01	4.36	7.13	7.53	4.59	5.73	2.91
Density (grams/cm)	0.72	0.88	0.84	0.90	0.95	1.00	0.93	0.72
Water absorption (by weight)	26%	30%	29%	35%	29%	24%	30%	61%

* These specimens spontaneously ruptured during soaking process.

Table 13. Comparison of Modulus of Rupture (MOR) Among LBWL Products and Several Refractory Materials

Material	Density (g/cm^3)	MOR (MPa)	Cold crushing strength (MPa)	Reference
LBWL product	0.89*	3.3*	5.3*	This study
Dry wall	0.72	1.9	2.9	This study
Insulating 92.5% SiO_2	0.95	0.9	1.2	[28]
1427 C Fireclay	0.79	1.1	0.9	[28]
1538 C Fireclay	0.92	1.3	1.6	[28]
1530 C High-alumina	0.90	3.4	6.9	[28]
High-alumina	0.95	0.9	1.1	[28]

* The data is an average value.

Table 14. Three Point Bend Testing of Reheated LBWL Product for Evaluating the Resistance to Water (unit: MPa)

Composition	1	2	3
MOR before reheating			
Testing at 25 C	3.37	2.37	3.57
Testing after soaking in water at 98 C for 2 hours	None*	0.56	0.75
MOR after reheating			
Testing at 25 C	2.17	1.29	2.32
Testing After soaking in water at 98 C for 2 hours	2.50	1.64	2.40

* These specimens ruptured spontaneously during soaking process.

(4) Examination of LBWL Product Reheated at Elevated Temperature

Abrasive wheels using aluminosilicate grains and a water glass binder can be made more water-resistant, though rather brittle, by firing between 850 degrees and 1100 degrees Celsius. In order to ascertain whether heating at 800-1150 degrees Celsius would affect the resistance of LBWL products to water attack, LBWL products were reheated at 800, 1000, and 1150 degrees Celsius respectively. The specimens reheated at 800 degrees Celsius were then tested in three point bend. Table 14 shows that reheating at 800 degrees Celsius can improve the water saturated strength of LBWL products, but the flexural strength of the reheated specimens decreases to about 60 percent of the original strength. The soaking process does not alter the flexural strength of the reheated LBWL product.

To understand why reheating the LBWL products can improve their resistance to water attack, the crystallographic phases present in the reheated LBWL product were analyzed using x-ray diffraction. The diffraction traces indicated that a new crystallographic phase occurred in composition 1 after it was reheated at 800 degrees Celsius. The new phase, or phases, are difficult to identify from the two new but weak x-ray diffraction peaks. When composition 1 was reheated at temperatures higher than 800 degrees Celsius, a new glassy phase appeared and gradually increased as the reheating temperature increased. Upon

heating to 1150 degrees Celsius, the glassy phase was predominant.

When specimens of composition 2 and 3 were reheated at 800 degrees Celsius, the crystallographic phases also changed, including the disappearance of the calcium carbonate phase. When the specimens were reheated at 1150 degrees Celsius, the x-ray diffraction peaks corresponding to mullite and quartz were no longer observable. In place of the mullite and quartz, a crystalline phase (or phases) appeared that had not been present at lower temperatures in the LBWL product. These phases have not yet been identified.

The bars of compositions 1, 2, and 3 partly melted upon reheating at 1150 degrees Celsius in air in an electrical resistance furnace. The liquid content in composition 1 was high enough to cause adjacent bars to fuse together and deform under their own weight. The softening of composition 2 was less than that for composition 1. The refractoriness of compositions 1, 2, and 3, and that of the fly ash may be ranked qualitatively as follows: fly ash > 2 > 3 > 1. As can be seen from Table 4, as the percentage of water glass in the LBWL product increases, the refractoriness of the product decreases.

In short, reheating LBWL products at 800 degrees Celsius leads to chemical reactions that promote water-resistance. Water glass is a good flux and thus will reduce the refractoriness of fly ash products. Partial melting may occur for temperatures in the neighborhood of 1150 degrees

Celsius. The proper addition of sludge will improve the refractory properties.

(5) Thermal Conductivity and Thermal Expansion

The hot-wire technique [29-31] has been recognized as a useful method for measuring the thermal conductivity of a refractory for several years. During the investigation, the conductivity test apparatus was carefully checked. The standard deviation of the conductivity data of the same specimen was approximately 11 percent.

The thermal conductivity of LBWL products is listed in Table 15. Figure 17 shows the thermal conductivities for compositions 1, 2, and 3. In each case, the conductivity increases almost linearly with increasing temperature. Table 16 compares the thermal conductivity of the LBWL products with seven commercial refractory materials. The dry wall received from Lansing Board of Water and Light has also been compared with the LBWL products. The dry wall has a lower thermal conductivity than the LBWL product, thus dry wall has somewhat better thermal insulation properties than the fly ash. Generally speaking, the thermal conductivity of LBWL products is similar to that of those refractory materials which have a mass density similar to that of the LBWL products.

At a given temperature, the thermal conductivity of the various LBWL product compositions is nearly identical.

Strictly speaking, LBWL products are not homogenous in structure. The location and the size distribution of pores are the main factors that influence thermal conductivity rather than the specific composition. For example, two different specimens of composition 1 have different values of thermal conductivity, 0.248 and 0.260 (watt / meter degrees Kelvin) respectively. A large pore in the center can give one specimen a dramatically lower thermal conductivity than another specimen which does not contain such a pore.

Thermal expansion is important for thermal shock and thermal spalling investigations. The thermal expansion of the LBWL products was measured using the Thermomechanical Analyzer (Model 9900 Du Pont Company, Wilmington, DE). The experimental data for compositions 1, 2, and 3 are illustrated in Figures 18A, 19A, and 20A respectively. If the LBWL products were tested prior to the "stablization" thermal anneal at 500 degrees Celsius, then the thermal expansion behaved in the irregular way shown in Figures 18B, 19B, and 20B. Typically, the thermal expansion of a solid shows the linear behavior illustrated in Figures 18A, 19A, and 20A. The extent of the departure from linearity for the thermal expansion curves for compositions 1, 2, and 3 (Figures 18, 19, and 20 respectively) corresponds to the calcium carbonate (sludge) content for that composition, as shown in Table 4 of the Experimental and Techniques section of this report. For example, composition 1 (Figure 18B) showed the least nonlinearity before the thermal stabilization treatment, and it is composition 1 that

contains the lowest fraction of sludge. Composition 2 has the highest sludge content and the highest nonlinearity in thermal expansion (Figure 19B) before thermal stabilization. Composition 3 is intermediate to 1 and 2, both in terms of the sludge content and in regard to the nonlinearity of the thermal expansion curve. The thermal expansion of the LBWL product is thus dependent upon both the composition and thermal history of the LBWL product.

Table 15. Thermal Conductivity of Various LBWL Products and Gypsum Board (Dry Wall)

Composition	Density (grams/cm^3)	Measuring temp. (degrees C)	Thermal conductivity (W/M.K)*
1	0.72	24	0.26
		196	0.33
3	0.84	23	0.25
		192	0.30
		303	0.31
		460	0.42
		580	0.39
4	0.90	23	0.27
		195	0.31
		301	0.34
		417	0.32
		511	0.36
		612	0.40
5	0.95	24	0.27
		196	0.33
6	1.0	23	0.27
		199	0.30
		301	0.33
		470	0.35
		560	0.36
7	0.93	23	0.26
		197	0.30
Dry wall	0.72	23	0.16

* (W/ M.K) : watt/ meter degree Kelvin.

Table 16. Comparison of Thermal Conductivity Among LBWL Products and Several Refractory Materials

Material	Density (g/cm^3)	Specific Heat (cal/g.C)	Thermal Conductivity (W/M.K)**	Reference
LBWL product	0.89*	0.192*	0.26*	This study
Dry wall	0.72		0.16	This study
Insulating brick	0.495	0.441	0.2	[3]
Insulating brick	0.93	0.441	0.4	[3]
Gypsum board	0.80	0.46	0.161	[35]
Masonry units CMU,6IN,LW, HOLLOW	0.88	0.37	0.481	[35]
Insulating 92.2% silica	0.949		0.31 (measured at 105 C)	[28]
1538 C Fireclay	0.916		0.29 (measured at 138 C)	[28]
1530 C High-alumina	0.900		0.26 (measured at 135 C)	[28]

* The data is an average value.
** (W/ M.K) : watt/ meter degree Kelvin.

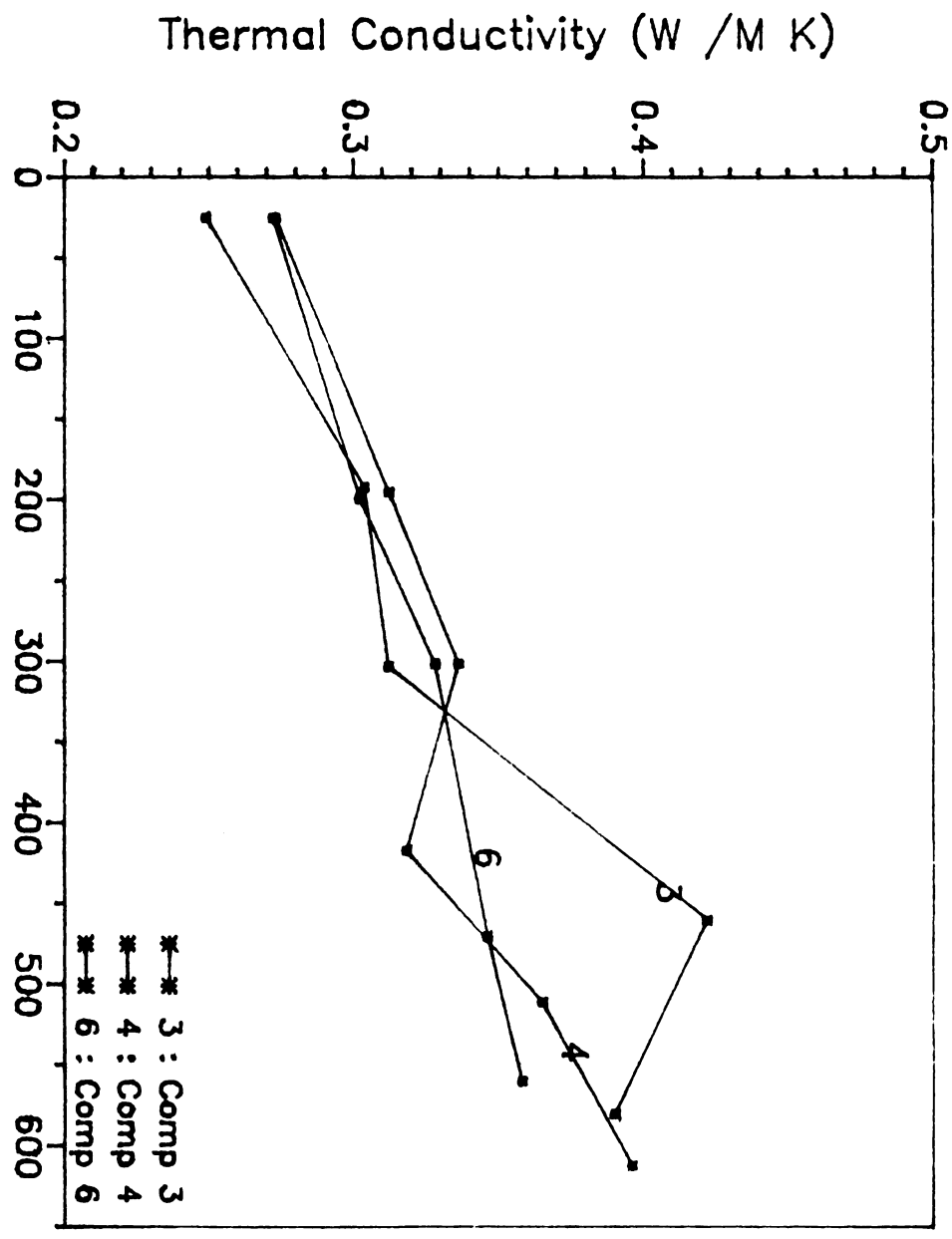

Figure 17 : Thermal Conductivity of LBWL Products

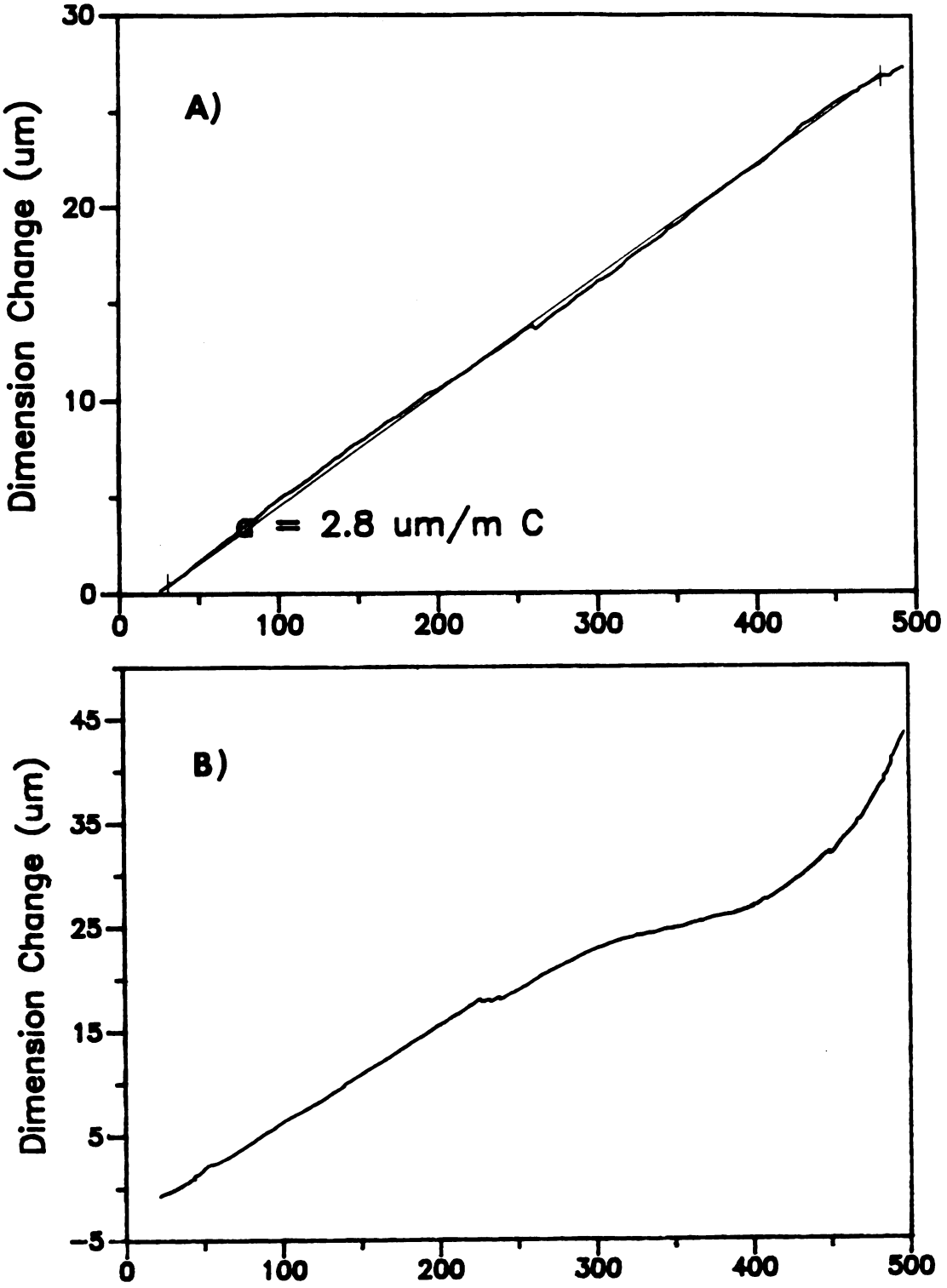

Figure 18. Thermal Expansion of Composition 1 of LBWL product
(A) After "Stabilization"
(B) Before "Stabilization"

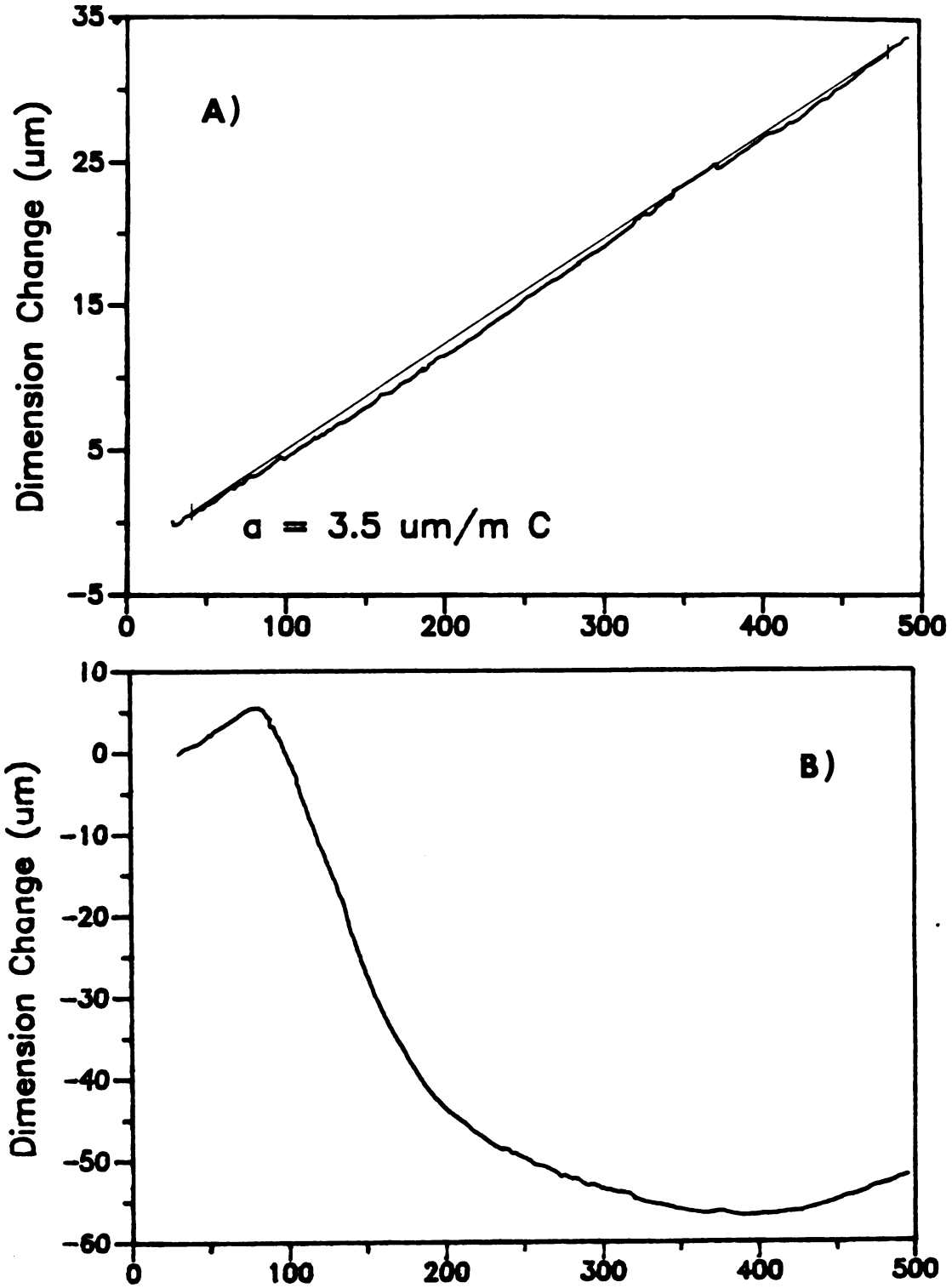

Figure 19.

Thermal Expansion of Composition 2 of LBWL product
(A) After "Stabilization"
(B) Before "Stabilization"

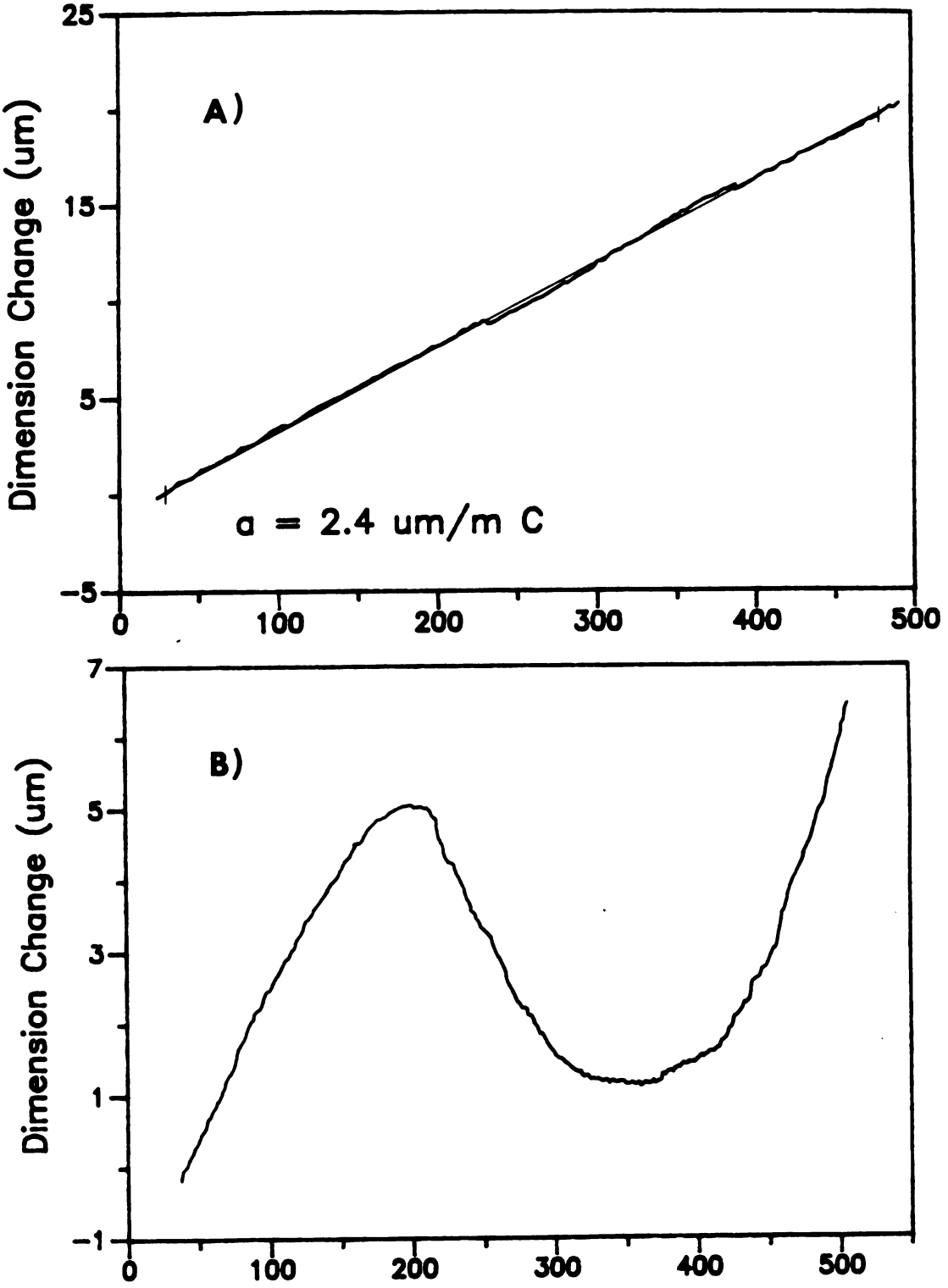

Figure 20.

Thermal Expansion of Composition 3 of LBWL product
(A) After "Stabilization"
(B) Before "Stabilization"

(6) Evaluation of Thermal Shock

When ceramic materials are subjected to a rapid change in temperature (thermal shock), microcracking or mechanical failure may occur. As a result, the materials exhibit a decrease in strength. For high-temperature applications, the thermal shock resistance is one of the main factors limiting the usefulness of ceramic materials.

LBWL products were heated in a furnace, quenched in air and then tested in three point bend to determine the thermal shock resistance parameter. The thermal shock resistance parameters for compositions 1, 2, and 3 are listed in Table 17. In comparison with the other refractories, the LBWL products seem to have a lower resistance parameter. Figure 21 illustrates that the bend strength of composition 1 does not decrease after thermal shock until the furnace temperature exceeds 630 degrees Celsius. (Recall that the thermal shock study depicted in Figure 21 involved quenching a heated specimen into room air at approximately 23 degrees Celisus.)

According to Hasselman's theory of thermal shock for brittle materials [4], a discrete transition in the residual strength occurs at a critical temperature (Figure 22). However, when compared to Figure 22, Figure 21 (for the LBWL product) shows a less dramatic transition in retained strength that commences at about 630 degrees Celsius, and in this way the thermal shock behavior observed for the LBWL product departs from the behavior predicted by Hasselman's

theory. In a study of the influence of the included porosity on the thermal shock behavior of polycrystalline alumina, Smith [34] found that porosity could lead to a behavior similar to that seen in Figure 21. Since the LBWL product is quite porous, the porosity may contribute to the lack of an abrupt transition in retained strength (after thermal shock), as predicted by Hasselman and as shown schematically in Figure 22. Regardless of the physical mechanisms involved, the strength of the LBWL product remains relatively unchanged for shock temperatures up to about 630 degrees Celsius, and for shock temperatures up to about 750 degrees Celsius there is relatively little drop off in the retained strength (Figure 21). This thermal shock behavior demonstrates that the LBWL product has sufficient thermal shock resistance to serve as a low duty refractory material (such as a furnace liner).

Table 17. The Comparison of Thermal Shock Resistance Parameter Among LBWL Products and Several Refractory Materials

Composition	LBWL product			Alumina refractory			Magnesite chrome refractory		
	1	2	3	1	2	3	1	2	3
Bulk density (g/cm^3)	0.72	0.88	0.84	2.55	2.58	2.60	3.2	3.1	3.03
Thermal expansion ($C * 10^{-6}$)	2.8	3.5	2.4	6.2	5.7	5.7	9.3	10	10.2
Elastic modulus (GPa)	4.3	3.5	5.4	13.5	10.5	32.5	41.3	20.7	20.9
Poisson's ratio	0.17	0.11	0.13	0.15	0.14	0.14			
Flexural strength (MPa)	3.26	2.15	3.0	9.8	9.7	17.3	6.89	3.93	4.41
Thermal shock resistance* (10^{-4} M /Joule)	50	89	60	1.6	1.4	1.3	10.3	16	7.9

* The thermal shock resistance parameters were evaluated using the ribbon test [36-37]

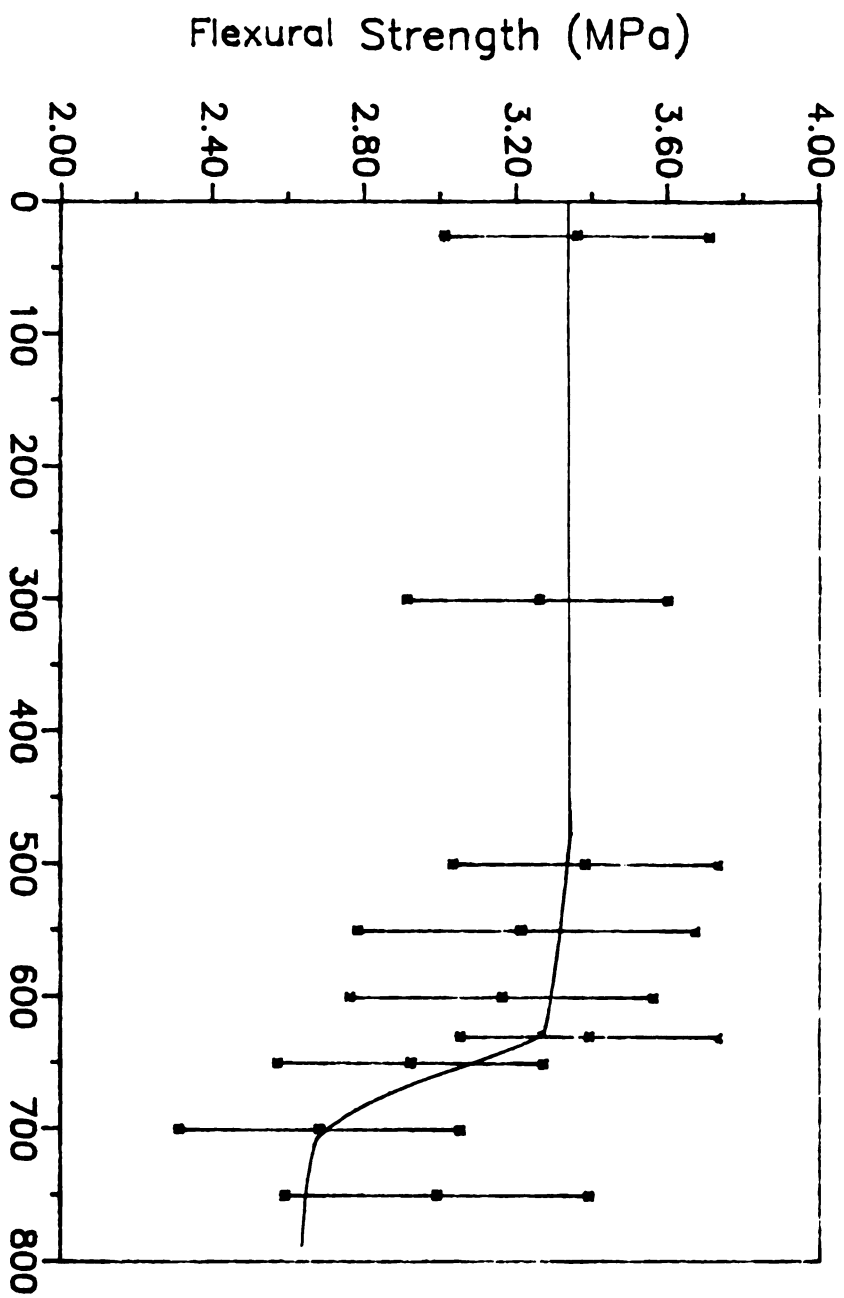

Figure 21. Strength behavior of LBWL product (composition 1) after thermal shock

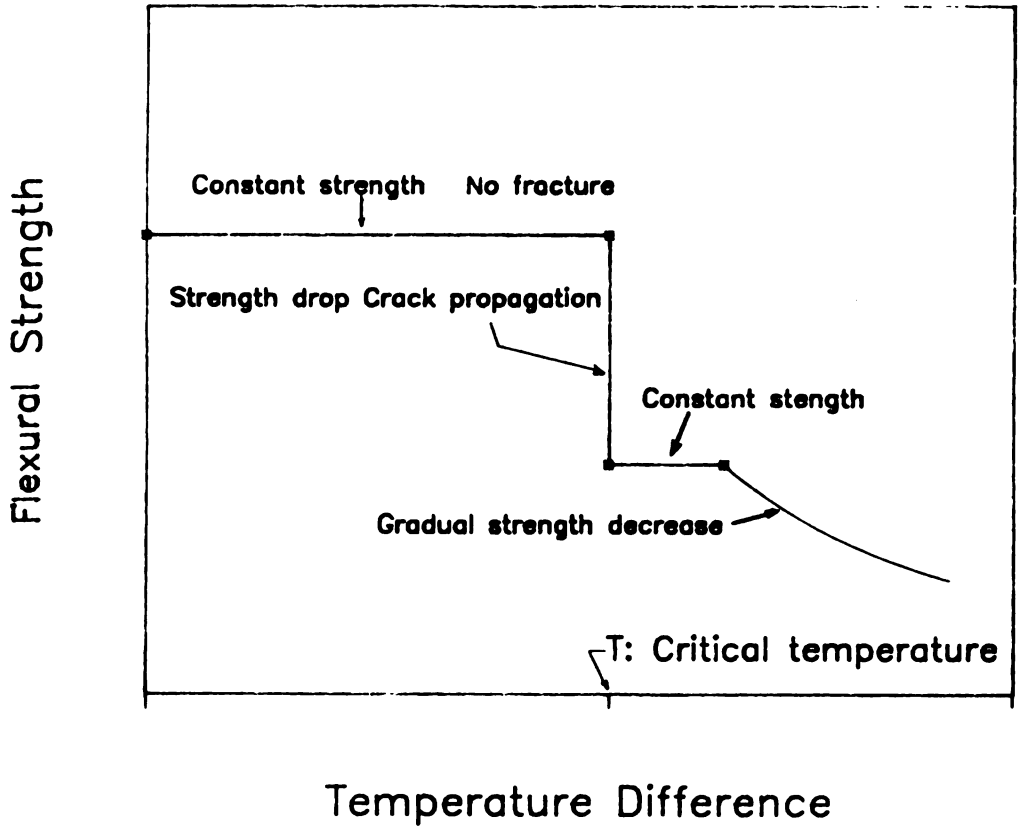

Figure 22. Schematic representation of strength behavior in brittle ceramics vs. severity of thermal shock as predicted by theory[4]

(7) Acoustic Damping Capacity

The vibrational response of a sound will always couple with the surrounding medium, which may commonly be air and wall. A wall composed of bricks having good acoustic damping capacity may lead to the noise emission and form an acoustic isolation.

The extent of acoustic energy dissipation in building brick or refractory can be evaluated by the measurement of the internal friction. In this work the fundamental flexural frequency was used as a standard reference frequency. The internal friction values for LBWL products and dry wall (gypsum board) are shown in Table 18. The LBWL products have higher internal friction than the dry wall. If the LBWL products are used as building material, they will have a better acoustic damping capacity than dry wall.

Table 18. The Internal Friction of LBWL Products and Dry Wall (Gypsum Board)

Composition	1	2	3	dry wall
Internal friction	0.0076	0.0049	0.0072	0.0022

CONCLUSIONS AND SUMMARY

The fly ash-calcium carbonate refractory materials (LBWL products) discussed in this report were formed from the Lansing Board of Water and Light by-products of fly ash and limestone sludge. X-ray diffraction analysis indicated that the major phases in the Board of Water and Light fly ash powder were mullite, quartz, and a glassy phase (Table 9). The primary phases of the limestone sludge were found to be calcium carbonate and magnesium hydroxide (Table 8 and Appendix A). Optical microscopy and scanning electron microscopy showed that the majority of the fly ash particles were spherical and approximately 5 to 40 microns in diameter (Figures 7-10).

The mechanical properties of the LBWL product are significantly affected by the phase composition and the particle size of the ingredients such as the fly ash, sludge, and the water glass that comprise the LBWL product. For example, the addition of water glass* to the LBWL product lowers the melting point of the LBWL product, so that the maximum use temperature for the LBWL product is about 1100 degrees Celsius. However, even without the water glass additions, the glassy phase inherent in the fly ash powders would limit the maximum use temperature to about 1200 to 1250

degrees Celsius for any product containing a substantial amount of fly ash. On the other hand, the water glass addition acts as a binding phase, which allows the LBWL product to be processed at the low temperatures (about 220 to 270 degrees Celsius) that can be obtained during microwave processing. During microwave processing, the fly ash serves as an inert filler bound together by the water glass phase. If no water glass were added, the small particle size of the fly ash powder makes it possible to sinter the fly ash at elevated temperatures, such as in a furnace at temperatures in excess of 1100 degrees Celsius. This sintering of fly ash powders could be used instead of microwave processing, but the high temperature processing would be economically unfavorable, compared to the relatively energy-efficient microwave processing technique.

The addition of sludge and phosphate to the LBWL products did not dramatically improve their mechanical properties. For example, sludge and phosphate decreased the ultimate flexural and compressive (cold crushing strength) of the LWBL product (Table 12 and Figure 15). Sludge additions increased the LBWL product's resistance to water attack, while phosphate additions gave no improvement (Figure 16).

As is typical of refractory materials, the flexural strength of the LWBL products decreased at elevated temperatures (Figure 14). Reheating the LBWL products at temperature exceeding about 800 degrees Celsius promoted the resistance to water attack, probably due to the additional

phases (including an enhanced glassy phase) that appear upon reheating at high temperatures.

The mechanical and thermal properties of the LBWL product generally compare quite favorably with both commercial low-duty refractory materials and with gypsum board (dry wall). Thus if economical and reliable production techniques can be developed, two potential uses for the LBWL products are as building materials (as a replacement for gypsum board) and as a low-duty refractory material. The flexural strength of the LBWL products ranged from about 2.37 MPa to 4.06 MPa. The compressive strength (cold crushing strength) ranged from 3.61 MPa to 7.53 MPa. For all of the LBWL products, the thermal conductivity was about 0.26 watt/meter degree Kelvin. The similarity among the thermal conductivities evidently stems from the fact that the thermal conductivity of a refractory material is dominated by the contribution to thermal conductivity due to the gas in the materials pores. Since each of the LBWL products has a similar total volume fraction porosity, the resulting thermal conductivities among the various LBWL compositions were quite similar.

The thermal expansion of the LBWL product was determined to be approximately $2.9 * 10^{-6}$ per degree Celsius. The thermal expansion behavior, however, can be dependent upon both the composition and the thermal history of the LBWL product (Figures 18-20). For example, for compositions containing calcium carbonate (sludge), the first heating of the LBWL product produced a thermal expansion curve that

first had a positive slope, then went through a maximum, and finally regained a positive slope (Figures 19 and 20). Heat treatment of these calcium carbonate bearing compositions at 500 degrees Celsius for about 48 hours produced a "stabilization" of the thermal expansion curve, in that the thermal expansion showed a positive, nearly constant slope over the entire range of test temperatures. (A shorter heat treatment at a higher temperature will probably produce similar stablization effects, but only the 500 degree Celsius, 48 hour stablization treatment was actually performed.) The observed changes in thermal expansion behavior with thermal history could be crucial if calcium carbonate containing products were used in large walls as low duty refractory bricks. The changes in the thermal expansion values could lead to extensive cracking during the first few times the refractories were heated, unless they had been properly "stabilized" by a preheating treatment before their first use in a refractory wall, such as might be the case in a large furnace.

In addition, LBWL products have higher mechanical strength, better water-resistance, higher thermal stability and better acoustic damping capacity than gypsum board (dry wall). However, gypsum board is a better thermal isulator than LBWL products. The thermal conductivity of gypsum board is 0.16 (watt/ meter degree Kelvin).

Appendix A

Quantitative Evaluation of $CaCO_3$ and $Mg(OH)_2$ in the Sludge Powder

The x-ray diffraction traces of sludge powders received from Lansing Board of Water and Light showed evidence of only two crystalline phases, $CaCO_3$ and $Mg(OH)_2$. In order to determine quantitatively the relative fraction of the two phases in the sludge powder, the external standard method of quantitative x-ray phase analysis was used [38-39]. The external standard method involves the comparison of the x-ray diffraction trace for the powder sample being studied with the x-ray diffraction trace for a standard powder specimen. In this case, the standard powder specimen was a pure $CaCO_3$. Since the sludge is a simple binary mixture, to within the limits of resolution of the x-ray diffraction unit, the external standard method is appropriate.

Equation A1 permits quantitative analysis of a two-phase mixture [38].

$$\frac{Ic}{Icp} = \frac{Wc\ (Uc/Pc)}{Wc\ (Uc/Pc - Um/Pm) + Um/Pm} \qquad (A1)$$

Ic = the intensity of the selected line of the $CaCO_3$ in the diffraction traces of sludge.

Icp = the intensity of the selected line of the $CaCO_3$ in the diffraction traces of pure $CaCO_3$.

Wc = the weight fraction of $CaCO_3$ in sludge.

Uc/Pc = the mass absorption coefficient of $CaCO_3$.

Um/Pm = the mass absorption coefficient of $Mg(OH)_2$.

The theoretically calculated values of the mass absorption coefficients for $CaCO_3$ and $Mg(OH)_2$ are 74.4 cm/gm and 23.1 cm/gm [38], respectively. From the measured intensities of selected $CaCO_3$ x-ray diffraction peaks, the intensity ratio Ic/Icp was determined to be 0.85. Using equation A1 and the experimental value of Ic/Icp, the weight fraction of $CaCO_3$ in the sludge was calculated as 0.65. The remaining 0.35 weight fraction of the sludge can be assumed, to a first approximation, to consist of $Mg(OH)_2$ powders. It should be noted, however, that the lower limit of resolution of an x-ray diffraction determination of the phase of a given powder is about 0.05. Thus, any minor phases that comprise about 5 percent or less of the total mass of the powder specimen will not be evident in a x-ray diffraction trace.

LIST OF REFERENCES

1) J. L. Gregg, Aresenical and Argentiferous Copper, The Chemical Catalog Company Inc., New York, 1934.

2) J. G. Vail, Soluble Silicates in Industry, The Chemical Company Inc., New York, pp. 166-209, 1928.

3) P. Jeschke, "Thermal Conductivity of Refractories: Working with the Hot-Wire Method", American Society for Testing and Materials, STP 660, pp. 172-185, 1978.

4) D. P. H. Hasselman, "Unified Theory of Thermal Shock Fracture Initiation and Crack Propagation in Brittle Ceramics", Journal of the American Ceramic Society, Vol. 52, pp. 600-604, 1973.

5) D. P. H. Hasselman, "Analysis of Thermal Stress Resistance of Microcracked Brittle Ceramics", Bulletin of the American Ceramic Society, Vol 58, pp. 856-603, 1979.

6) T. K. Gupta, "Strength Degradation and Crack Propagation in Thermally Shocked Alumina", Journal of the American Ceramic Society, Vol. 55, pp. 249-253, 1976.

7) W. D. Kingery, Introduction to Ceramics, John Wiley & Sons Inc., New York, 1976.

8) E. Schreiber, O. L. Anderson and N. Soga, Elastic Constants and Their Measurement, McGraw-Hill, New York 1974.

9) J. B. Wachtaman, "Effect of Suspension Position on Apparent Values of Internal Friction Determined by Forster's Method", The Review of Scientific Instruments, Vol. 29, pp. 517-520, 1958.

10) The Condensed Chemical Dictionary, 9th edition, Van Nostrand Reinhold Company, New York, 1977.

11) G. J. McCarthy, Editor, Fly Ash and Coal Conversion By-Products: Characterization, Utilization, and Disposal. I, Material Research Society, pp. 1-66, 1985.

12) S. V. Mattigod, "Scheme for Density Separation and Identification of Compound Forms in Size-Fractionated Fly Ash", Fuel, Vol. 62, pp. 927-931, 1983.

13) R. S. Mitchell, "Mineralogy of Ash of Some American Coals: Variations with Temperature and Source", Fuel, Vol.55, pp. 90-96, 1976.

14) R. C. Joshi, "Pozzolanic Activity in Synthetic Fly Ashes: I, Experimental Production and Characterization", Bulletin of the American Ceramic Society, Vol. 52, pp. 456-458, 1973.

15) L. D. Hansen, "Crystalline Components of Stack-Collected, Size-Fractionated Coal Fly Ash", Environmental Science & Technology, Vol. 15, pp. 1057-1062, 1981.

16) G. L. Fisher, Bruce A. Prentice, David Silberman, John M. Ondov, and Arthur H. Biermann, "Physical and Morphological Studies of Size-Classified Coal Fly Ash", Environmental Science & Technology, Vol. 12, pp. 447-451, 1978.

17) M. Anderson, "The Benefication of Power Station Coal Ash and its Use in Heavy Clay Ceramics", Transactions and Journal of the British Ceramic Society, pp. 50-55, 1983.

18) R. J. Lauf, "Cenospheres in Fly Ash and Conditions Favouring their Formation", Fuel, Vol. 60, pp. 1177-1179, 1981.

19) R. J. Lauf, "Microstructures of Coal Fly Ash Particles", Ceramic Bulletin, Vol. 61, pp. 487-490, 1982.

20) W. R. Morgan, "Mechanism of the Hardening of Clay-Sodium-Silicate Mixture", Journal of the American Ceramic Society, Vol. 23, pp. 170-173, 1940.

21) G. W. Morey, "The Bond in Ceramics", Journal of the American Ceramic Society, Vol. 17, pp. 145-155, 1934.

22) H. L. Bolton, "Soluble Silicate and the Refractory Industry", Bulletin of the American Ceramic Society, Vol. 27, pp. 229-234, 1948.

23) A. E. Currier, "Influence of Sodium Silicate Composition on its Behavior with Sodium Carbonate as a Casting Slip Deflocculant", Journal of the American Ceramic Society, Vol.26, pp. 67-71, 1943.

24) G. Y. Onoda, Jr., "Theoretical Strength of Dried Green Bodies with Organic Binders", Journal of the American Ceramic Society, Vol. 59, pp. 236-239, 1976.

25) J. E. Comeforo, "Wetting of Al_2O_3-SiO_2 Refractories by Molten Glass: II, Effect of Wetting on Penetration of Glass into Refractory", Journal of the American Ceramic Society, Vol. 35, pp. 142-148, 1952.

26) R. A. Heindl, "Effect of Water Content and Mixing Time on Properties of Air-Setting Refractory Mortars Containing Sodium Silicate", Bulletin of the American Ceramic Society, Vol. 19, pp. 430-434, 1940.

27) H. R. Thornton, "Bond Strength and Elastic Properties of Ceramic Adhesives", Journal of the American Ceramic Society, Vol. 45, pp. 201-209, 1962.

28) William J. Smothers, Editor, Ceramic Source, American Ceramic Society Inc., Columbus, OH, Vol. 1, pp. 355-359, 1985.

29) H. A. Fine, "Analysis of the Applicability of the Hot-Wire Technique for Determination of the Thermal Conductivity of a Diathermanous Materials", American Society for Testing and Materials, STP 660, pp. 147-153, 1978.

30) A. J. Jackson, "Thermal Conductivity Measurements on High-Temperature Fibrous Insulations by the Hot-Wire Method", American Society for Testing Materials, STP 660, pp. 154-171, 1978.

31) W. R. Davis, "Determination of the Thermal Conductivity of Refractory Insulating Materials by the Hot-Wire Method", American Society for Testing Materials, stp 660 pp. 186-199, 1978.

32) P. Prelovsek, "Generalized Hot-Wire Method for Thermal Conductivity Measurements", Journal of Physics E : Scientific Instruments, Vol. 17, pp. 674-677, 1984.

33) G. D. Morrow, "Improved Hot-Wire Thermal Conductivity Technique", Bulletin of the American Ceramic Society, Vol. 58, pp. 687-690, 1979.

34) R. D. Smith, "Influence of Induced Porosity on the Thermal Shock Characteristics of Alumina", Bulletin of American Ceramic Society, Vol. 55, pp. 979-982, 1976.

35) D. E. Cory, Handbook of Thermal Insulation Applications, Noyes Pub., Park Ridge, NJ pp. 88-89, 1984.

36) C. E. Semler, "Thermal Shock of Alumina Refractories", Bulletin of the American Ceramic Society, Vol. 60, pp. 724-729, 1981.

37) C. E. Semler, "Thermal Shock Damage of Magnesite Chrome Refractories in the Ribbon Test", Bulletin of American Ceramic Society, Vol. 63, pp. 605-609, 1984.

38) B. D. Cullity, Elements of X-Ray Diffraction, Addison-Wesley Publishing Co., Reading, Massachusetts, PP. 407-411, 1974.

39) G. W. Brindley, Crystal Structure of Clay Minerals and Their X-ray Identification, Mineralogical Society, 41 Queen's Gate, London SW7 5HR, pp. 411-417, 1980.